Journal of Medicinal Chemistry

Drug Annotation

Discovery and Early Clinical Development of an Inhibitor of 5-Lipoxygenase-Activating-Protein (AZD5718) for Treatment of Coronary Artery Disease

Daniel Pettersen, Johan Broddefalk, Hans Emtenäs, Martin A Hayes, Malin Lemurell, Marianne Swanson, Johan Ulander, Carl Whatling, Carl Amilon, Hans Ericsson, Annika Westin Eriksson, Kenneth Granberg, Alleyn T. Plowright, Igor Shamovsky, anita dellsén, Monika Sundqvist, Mats Någård, and Eva-Lotte Lindstedt

J. Med. Chem., **Just Accepted Manuscript** • DOI: 10.1021/acs.jmedchem.8b02004 • Publication Date (Web): 14 Mar 2019

Discovery and Early Clinical Development of an Inhibitor of 5-Lipoxygenase-Activating-Protein (AZD5718) for Treatment of Coronary Artery Disease

Daniel Pettersen[†], Johan Broddefalk[†], Hans Emtenäs[‡], Martin A. Hayes[‖], Malin Lemurell[†], Marianne Swanson[†], Johan Ulander[‡], Carl Whatling[†], Carl Amilon[†], Hans Ericsson[#], Annika Westin Eriksson[§], Kenneth Granberg[†], Alleyn T. Plowright[†¥], Igor Shamovsky[£], Anita Dellsèn[‖] Monica Sundqvist[†¥], Mats Någård[†], Eva-Lotte Lindstedt[†]*

[†]Cardiovascular, Renal and Metabolism IMED Biotech Unit; [‡]Pharmaceutical Sciences IMED Biotech Unit [‖]Discovery Sciences IMED Biotech Unit; [#]Early Clinical Development IMED Biotech Unit; [§]Drug Safety and Metabolism IMED Biotech Unit; [£]Respiratory, Inflammation and Autoimmunity IMED Biotech Unit; AstraZeneca, SE-43183 Gothenburg, Sweden.

[¥] See Present Address.

KEYWORDS: FLAP, 5-lipoxygenase activating protein, inhibitor, 5-LO pathway, Leukotriene B_4, LTB_4, Leukotriene E_4, LTE_4, AZD5718, inflammatory disease, coronary artery disease (CAD).

ABSTRACT: 5-lipoxygenase activating protein (FLAP) inhibitors attenuate 5-lipoxygenase pathway activity and reduce the production of pro-inflammatory and vasoactive leukotrienes. As such, they are hypothesized to have therapeutic benefit for the treatment of diseases that involve chronic inflammation including coronary artery disease. Herein, we disclose the medicinal chemistry discovery and the early clinical development of the FLAP inhibitor AZD5718 (**12**). Multiparameter optimization included securing adequate potency in human whole blood, navigation away from Ames mutagenic amine fragments whilst balancing metabolic stability and PK properties allowing for clinically relevant exposures after oral dosing. The superior safety profile of AZD5718 compared to earlier frontrunner compounds, allowed us to perform a Phase 1 clinical

study in which AZD5718 demonstrated a dose dependent and greater than 90% suppression of leukotriene production over 24 h. Currently, AZD5718 is evaluated in a Phase 2a study for treatment of coronary artery disease.

Introduction

The 5-lipoxygenase (5-LO) pathway is responsible for the production of leukotrienes, lipid mediators derived from arachidonic acid that have inflammatory and vasoactive actions and that are involved in the innate immune response.[1, 2] The pathway is primarily expressed by a subset of white blood cells including neutrophils, eosinophils, monocyte/macrophages, and mast cells. Biological actions of leukotrienes include stimulation of leukocyte chemotaxis, neutrophil activation, promotion of vasopermeability and vasoconstriction.

The formation of leukotrienes involves oxidation of membrane-released arachidonic acid by 5-LO to the unstable intermediate Leukotriene A_4 (LTA_4) that can subsequently be converted via Leukotriene A_4 Hydrolase to Leukotriene B_4 (LTB_4) or via Leukotriene C_4 Synthase to leukotriene C_4 (LTC_4) (Figure 1). LTC_4 may subsequently be converted to

leukotriene D_4 (LTD_4) and the end-metabolite leukotriene E_4 (LTE_4) by the action of different peptidases.

FLAP (5-lipoxygenase activating protein) is critical for the production of leukotrienes by intact cells. Under resting conditions 5-LO is located in the cytoplasm but following an inflammatory stimulus and release of intracellular calcium it can translocate to the nuclear membrane where it interacts with FLAP. FLAP facilitates the transfer of arachidonic acid released from membrane phospholipids to the active site of 5-LO to initiate the production of leukotrienes.

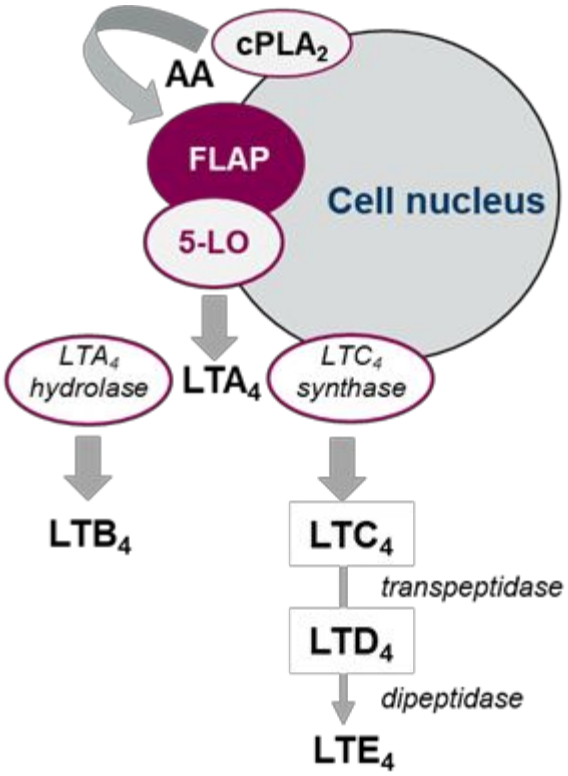

Figure 1. The 5-lipoxygenase pathway and the biosynthesis of leukotrienes. FLAP is located in the nuclear membrane and mediates transfer of the arachidonic acid substrate (AA) to the active site of 5-LO. $cPLA_2$, cytosolic phospholipase A2.

The 5-LO pathway has been a target for drug development for a number of diseases in which chronic inflammation is involved in the pathophysiology. This includes respiratory diseases such as asthma and chronic obstructive pulmonary disease (COPD), but also cardiovascular diseases such as atherosclerotic coronary artery disease (CAD).[3] Of particular interest, treatment with the 5-LO inhibitor VIA-2291 for 6 months resulted in an

improvement in cardiovascular parameters in CAD patients that had experienced an acute coronary syndrome (ACS) event around 1 month prior to treatment start.[4, 5] This included evidence of reduced coronary lesion formation and improvement in left ventricular ejection fraction (LVEF). On the other hand, in a separate study run as part of the same Ph2 program, VIA-2291 did not reduce arterial inflammation in an index vessel measured indirectly by FDG-PET.[6] Based on this limited clinical experience, more studies are required to fully address whether 5-LO pathway inhibition can have a therapeutic benefit in CAD patients.

Inhibition of leukotriene production can be achieved by targeting either 5-LO or FLAP to block the generation of the leukotriene precursor LTA_4.[7, 8] FLAP may be a particularly attractive drug target since FLAP inhibitors block activity of the 5-LO pathway at the initial step of leukotriene production. Moreover, it has been suggested that FLAP inhibition might deliver a more robust and sustained suppression of 5-LO pathway activity *in vivo* than can be achieved by 5-LO inhibition itself.[9]

FLAP inhibitors were first studied in human clinical trials in the 1990s. Following the initial clinical studies, a number of more recent compounds have entered clinical trials or have been proposed as clinical candidates.[10-13] However, no FLAP inhibitor has progressed beyond Phase 2 clinical trials. To date, most of the FLAP inhibitors that have entered into clinical development, including AM803[11], have originated from the chemical series exemplified by MK-591[14, 15] (Figure 2). Development of compounds based on this compound series were stopped due to safety concerns, low efficacy or sub-optimal ADME properties.[10] AstraZeneca's earlier explorations of FLAP inhibitors led to the clinical candidate AZD6642 that due to cardiovascular safety concerns, *vide infra*, did not progress to clinical evaluation.[16]

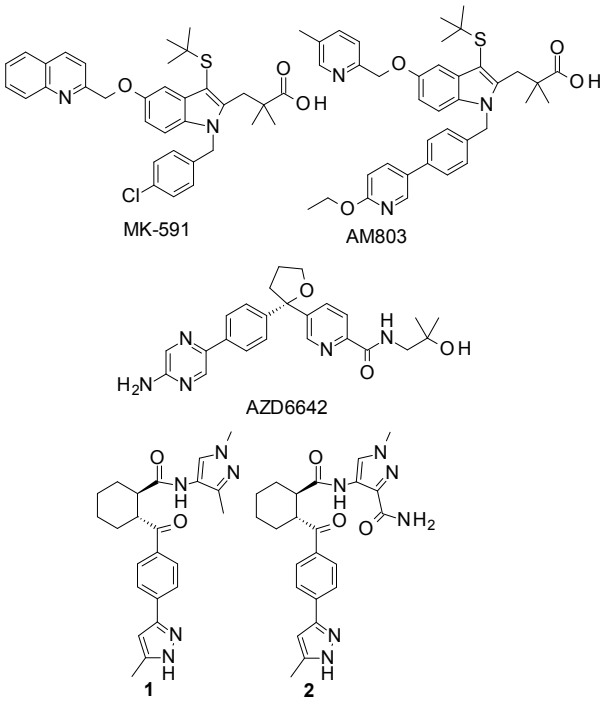

Figure 2. FLAP inhibitors

We recently published details of a novel chemical series of FLAP inhibitors, with two representative compounds (**1** and **2**) depicted in Figure 2.[17] Compound **1** was shown to be a potent FLAP inhibitor with potency and pharmacokinetic (PK) properties suitable for further preclinical testing. As such, **1** was subjected to 14-day rat and dog toxicity studies as well as a dog cardiovascular telemetry study. To our disappointment, administration of compound **1** increased heart rate, blood pressure and cardiac contractility in dogs and provoked coronary arteritis with a 20-fold estimated margin between NOAEL (No

Observed Adverse Effect Level) and predicted plasma exposure in humans at an efficacious dose (*vide infra*). An association between arteritis and heart rate could be observed on a group level but the increases in heart rate on an individual level were small. Even though the mechanisms behind the cardiovascular effects for AZD6642 and **1** may be different, both compounds induced heart rate increases in dogs. Despite detailed investigations, the mechanism behind the increases in heart rates is still unknown and no *in vitro* signal could be identified. To our knowledge, previous FLAP compounds have not been reported to have general cardiovascular safety concerns and even though compound **1** displayed sub-optimal cardiovascular safety *in vivo*, its cardiovascular safety profile was better than AZD6642. This suggested that the observed safety concerns were not due to inhibition of FLAP *per se*. We therefore decided to continue lead optimization with the aim of identifying a compound with improved potency and metabolic stability and, as a result, a lower predicted human dose and increased safety margin. Moreover, the desired candidate drug target profile demanded a compound without any significant effects on functional cardiovascular parameters, with a focus on heart rate, and a 100-fold margin to the predicted free maximum concentration, C_{max}, in human. To confirm lack

of treatment related histopathology findings, such as coronary arteritis, selected compound was subjected to a thorough *in vivo* safety profiling in repeated dose toxicology studies.

The structure-activity relationship (SAR) previously generated for this chemical series provided insights and learnings that were beneficial for further optimization.[17] For example, metabolism of the cyclohexyl core via cytochrome P450 (CYP450) metabolism proved problematic and this could be mitigated by reducing lipophilicity (log D < 3.0). The presence of the ketone functionality initially caused some concern due to its potential electrophilic and reactive nature. However, no or low levels of adducts using nucleophiles such as cyanide, glutathione or methoxylamine, with and without pre-incubation in human microsomes, were observed for this chemical series indicating no increased risk for reactive metabolite formation. In addition, the early SAR data generated indicated that the amino-pyrazole fragment heavily impacted the potency, lipophilicity and metabolic stability of the compounds and it was therefore decided to focus our optimization efforts on that specific moiety. As there were no high-resolution crystal structures available for

the FLAP protein, the optimization work at this stage was driven mainly by structure-activity and structure-property relationships and ligand-based strategies.[14, 18] As part of our screening and profiling cascade we utilized a competition binding assay using ^{3}H-MK-591 as the tracer[19] followed by a human whole blood (hWB) assay to study the inhibition of the 5-LO pathway by measuring the levels of LTB_4 after calcium ionophore stimulation. To enable a comparison of the compounds intrinsic activity in the cellular system the potency was corrected for the protein binding to establish the free potency. In the human whole blood assay, we and others noticed a time course dependency, especially for poorly permeable compounds, and we therefore measured LTB_4 inhibition after a 4 h compound incubation.[11, 17] Besides cellular activity, metabolic stability in human hepatocytes and permeability in Caco-2 cells were key for compound optimization clearly motivating a multiparameter design approach to identify a clinical candidate. To select compounds to progress into further studies, an early dose to man prediction (eD2M) was used as a ranking tool. We aimed to inhibit the FLAP 5-LO pathway activity at 80% over a 24 h period and $3xIC_{50}$ in the hWB assay was used as the minimum efficacious concentration (C_{ss}) over 24 h. Predicted human clearance ($CL_{hum,\ pred}$) was scaled from

intrinsic clearance data (Cl_{int}) generated in human hepatocytes using well established methods (see Supporting Information for details). Bioavailability (F) was estimated considering hepatic first pass effects only, since absorption was predicted to be complete based on the high Caco-2 apparent permeability (P_{app}) values. Scaling factors, constants and equations for eD2M prediction are described in the Supporting Information.

Results and Discussion

When comparing compound **1** and the primary amide **2** we realized that the lipophilicity was alike for the two compounds despite **2** having a more polar substituent on the amino-pyrazole with compound **2** containing a primary amide and compound **1** containing a methyl substituent (Table 1). We hypothesized that the lipophilicity could be reduced, leading to higher metabolic stability, by moving the *N*-methyl substituent in the amino-pyrazole ring closer to the primary amide substituent forcing the primary amide slightly out of plane due to steric effects resulting in a more exposed primary amide. We were therefore pleased to see that compound **3** had a reduced lipophilicity value, as measured by log D (2.6 instead of 3.1) whilst maintaining a similar potency to **2** in the competition

binding assay (IC_{50} value = 35 nM). The increased polarity also translated to improved solubility and a higher metabolic stability in human and rat hepatocytes, with the permeability in the Caco-2 assay remaining at an acceptable level (Table 1) to reach a reasonable fraction absorbed in rat and dog PK experiments (data not shown). The overall improved properties for **3** resulted in the eD2M prediction to be considerably lower compared to previous compounds **1** and **2**. Elongating the *N*-methyl substituent on the amino-pyrazole ring to an ethyl group resulted in the equipotent derivative **4** suggesting that expansion in this direction was tolerated. However, the switch to an ethyl substituent in **4** caused an increase in log D relative to **3** and a dramatic increase in the eD2M prediction due to the reduced metabolic stability but retained potency. Instead we introduced a polar group such as an elongated primary amide to give compound **5**, which although active was significantly less active than **3**. We reasoned that the primary amide functionality was worth further explorations and as we had observed that modification of the angle between the amino-pyrazole ring and the primary amide substituent could have a large impact on both potency and lipophilicity (cf. compound **2** vs. **3**) we explored if the torsion angle between the amino-pyrazole ring in relation to the cyclohexyl carboxamide

bond could have a similar effect. As a result, a methyl group was introduced into the 3-position of the amino-pyrazole of **3** to give compound **6** which proved to have a very promising profile. The potency of **6** in the competition binding assay was slightly reduced (IC_{50} = 101 nM) but the free potency observed in the human whole blood assay was significantly improved (IC_{50} = 8.0 nM). The metabolic stability was also improved further compared to **3**, which resulted in a reduced eD2M prediction. We also prepared the primary amide **7** having no *N*-substitution on the amino-pyrazole ring, but this compound exhibited reduced metabolic stability in human and rat hepatocytes, despite its reduced lipophilicity compared to **3** and **6**.

Metabolic activation of primary aromatic and heteroaromatic amines, such as *N*-hydroxylation by P450 enzymes, primarily CYP1A2, and further formation of bioconjugates by Phase II enzymes, may lead to mutagenic and carcinogenic activity.[20, 21] Since hydrolysis of the cyclohexyl carboxamide motif would result in the release of primary amino-pyrazoles we were keen to understand their potential for mutagenic activity. Mutagenicity of the primary amino-pyrazoles was evaluated in an Ames bacterial mutagenicity assay in strains TA98 and TA100, with and without metabolic activation

using rat S9 fraction (Table 1).[22] As part of our project strategy we decided to not progress any FLAP inhibitors having an Ames positive masked amino-pyrazole moiety. To our disappointment we realized that several of the amino-pyrazoles were Ames mutagenic, thus having an increased risk for carcinogenic activity. For example, the corresponding amino-pyrazoles in **3** and **6** where both Ames mutagenic. There are reports suggesting that genotoxicity of aromatic amines is influenced by their geometric fit to the active site of CYP1A2 and stability of the anionic intermediates[23, 24] as well as by the chemical reactivity of hydroxylamines and their bioconjugates for DNA basepairs under slightly acidic conditions.[25] Therefore, modulation of the electronic character and steric effects of the amino-pyrazoles could be one way to modulate genotoxicity. However, due to little genotoxicity data being available for amino-pyrazoles used in the chemical series we could not verify this hypothesis. We were instead pleased to see some of the amino-pyrazoles tested to be negative in the Ames test indicating that Ames negative aromatic amines could be identified within the scope of this chemical series and we adopted the Ames test of the amino-pyrazoles as part of our screening strategy going forward.

To build our understanding further we investigated if other polar groups could be used to replace the primary amide on the amino-pyrazole ring. The carboxylic acid **8** and the hydroxamic acid **9** both displayed good FLAP binding activity but the potency in the human whole blood assay was reduced, even if protein binding was compensated for. As a consequence of their high polarity the acids did not display sufficient Caco-2 permeability, but the data suggested that various polar motifs were tolerated in this area of the molecule from a potency perspective. To modulate the permeability of **9** we evaluated less polar and alkylated hydroxamic acids such as **10** which displayed high potency in both the competition binding assay and in the human whole blood assay in combination with good Caco-2 permeability, even at the expense of a somewhat reduced ligand lipophilicity efficiency (pIC_{50} hWB_{free} - $LogD_{7.4}$). The chemical stability for the hydroxamic ether **10**, containing an *O*-tBu residue, was surprisingly high and no chemical decomposition was observed at pH 1, 7 or 10. In addition, **10** was found to be metabolically stable and no cleavage of the hydroxamic ether could be identified in rat or human hepatocytes. The sulfonamide **11** also displayed high binding affinity (IC_{50} = 34 nM) which translated into good inhibition of LTB_4 production in the human whole blood

assay. Following the promising profiles of **10** and **11**, both compounds displayed low eD2M predictions and gratifyingly the amino-pyrazoles in the hydroxamic ester **10** and sulfonamide **11** were found to be Ames negative.

Overall, the SAR data suggested that the use of polar moieties in the 2-position of the amino-pyrazole such as primary amides, carboxylic acids, sulfonamides and other polar groups (not listed here) were well tolerated from a potency perspective. However, analyzing the overall profile and the eD2M predictions, the primary amides **3** and **6** had preferred profiles but failed the screening criteria as they contained Ames mutagenic amino-pyrazoles. We expected the amino-pyrazoles in **3** and **6** to have some flexibility and rotational character around the primary amide bond leading to some degree of conformational freedom. To reduce the conformational degrees of freedom, the more conformationally restricted bicyclic amino-pyrazole **12** (AZD5718) was made, which demonstrated good FLAP binding affinity displaying an IC_{50} value of 6.0 nM. Compound **12** also showed excellent potency in inhibiting LTB_4 production in the human whole blood assay (IC_{50free} value = 2.0 nM). Overall, compound **12** displayed a promising profile from a metabolic stability and Caco-2 permeability perspective which was reflected in the

reduced eD2M prediction and we were pleased to see the corresponding amino-pyrazole contained in compound **12** to be Ames negative.

Table 1. Profiling of compounds **1-12**.

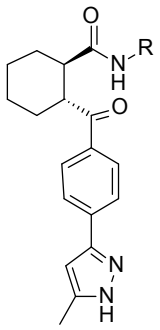

Amino-pyrazole (-NR) Cmpd	LogD[a]	Solub Aq. (μM)	FLAP Bind[b]/ hWB[c]$_{free}$ (IC_{50} nM)	LLE[d] hWB$_{free}$	Hep.Clint[e] h/r (μL/min/ 10^{-6} cells)	Papp[f] Caco2 1E-6.cm/s	eD2M[g] mg/day OD	Ames[h] 2-strain (amino-pyrazole)
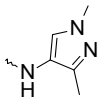 **1**	3.1	225	59/7.4	5.1	4.0/12.8	20.5	1900	NEG
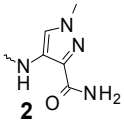 **2**	3.1	60	36/22	4.6	12.4/14.0	22.0	>18000	NEG
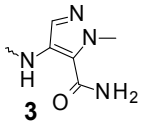 **3**	2.6	475	35/13	5.3	3.0/6.5	2.6	170	POS
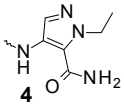 **4**	2.9	329	29/16	4.9	4.9/8.6	9.2	7800	POS
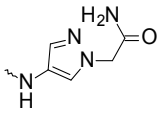 **5**	2.1	496	241/487	4.2	nd/nd	nd	3500	nd

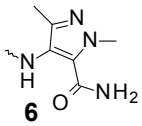 **6**	2.6	399	101/8.0	5.5	<1.0/5.7	1.4	34	POS
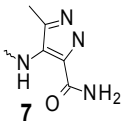 **7**	2.3	402	24/96	4.7	6.7/14.4	0.15	>18000	nd
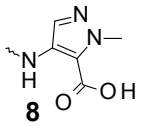 **8**	0.2	599	17/570	6.0	3.2/nd	0.21	>18000	nd
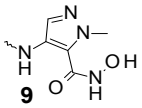 **9**	2.1	224	47/nd	-	nd/nd	nd	-	nd
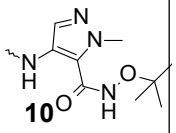 **10**	3.3	208	5.8/1.6	5.5	6.0/19.5	14.7	55	NEG
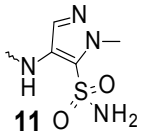 **11**	3.4	79.7	34/6.5	4.8	4.9/9.7	9.0	80	NEG
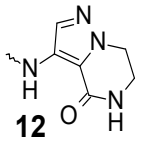 **12**	2.9	104	6.3/2.0	5.8	4.2/13.8	3.7	44	NEG

See Supporting Information for full details. [a]Octanol/water partition coefficient at pH 7.4, [b]IC_{50} in the FLAP competition binding assay, [c]Calculated as hWB IC_{50free} (IC_{50} in the human whole blood assay measuring the inhibition of the downstream LTB_4 production after 4 h incubation of the compound) × (compound's unbound fraction in human plasma (Fu) /100). Fu = 100-human protein binding(%). [d]LLE calculated from pIC_{50} hWBfree minus LogD7.4. [e]Intrinsic clearance of compounds after incubation in human or rat hepatocytes. [f]Passive permeability measured in Caco-2 cells in the A to B direction, pH=6.5 [g]Early dose to man prediction based on 3xIC_{50} hWB coverage for 24 h. [h]2 strain Ames test with and without metabolic activation using rat S9. nd = not determined.

Based on the overall properties and the eD2M predictions, compounds **10**, **11** and **12** were selected for further profiling. The eD2M prediction, albeit preliminary, indicated a significant lowering of the human dose which potentially could lead to higher safety margin for compounds **10**, **11** and **12** relative to our previous frontrunner **1**.

Generally, in this chemical series no issues were observed with inhibition of CYP450 enzymes and compounds **10** to **12** did not inhibit any of the isoforms 1A2, 2C8, 2C9, 2C19, 2D6 or 3A4 (IC_{50} values > 20 μM). No adducts could be seen for **10-12** using glutathione, cyanide or methoxylamine as trapping agents after compound incubation in human liver microsomes confirming the inert nature of their respective ketone moiety. Major metabolic elimination pathways in this series were CYP450 mediated hydroxylation in the cyclohexyl ring, ketone reduction, *N*-demethylation in the amino-pyrazole ring and, less frequently, hydrolysis of the cyclohexyl carboxamide.[17] The major metabolic pathways and contribution of CYP3A4 metabolism for compounds **10**-**12** are listed in Table 2. Compounds **10** and **11** were moderately dependent on CYP3A4 metabolism (66% and 68%, respectively) as seen by the relative contribution of CYP3A4 considering

a panel of six CYP isoforms 1A2, 2C8, 2C9, 2C19, 2D6 or 3A4. Compound **12** displayed a higher degree of CYP3A4 dependence (94%) indicating a potential risk for drug-drug interaction if co-medicated with a CYP3A4 inhibitor. The contribution of CYP3A4 mediated oxidation related to total metabolism was further investigated in hepatocytes as fraction metabolized by CYP3A4 using ketoconazole as the CYP3A4 inhibitor. The CL_{int} was reduced by 54% in incubations with ketoconazole in human hepatocytes, suggesting **12** to have a low risk as a victim due to drug-drug interactions. This was rationalized due to the pronounced alternative Phase 2 elimination pathways such as *N*-glucuronidation of the parent molecule **12**.

The *in vivo* PK characteristics of compounds **10**, **11** and **12** were assessed in the rat and the dog, Table 2. For compound **10**, the oral bioavailability in dog was high (65%) but lower in the rat (12%) and the half-life following *iv* administration was 4.7 and 7.0 h for rat and dog respectively. Compound **11** displayed similar PK properties in the dog, with a slightly higher volume of distribution and clearance, but a similar half-life to compound **10**. A somewhat higher clearance in the rat contributed to a shorter half-life in rat compared

to the dog than what was observed for compound **10**. For compound **12**, the bioavailability was in line with **10** and **11** in the dog. However, a shorter half-life was observed following *iv* administration of compound **12** to the dog (2.1 h). A high clearance contributed to an even shorter half-life in the rat.

Table 2. ADME data for compound **10**-**12**.

Cmpd	PPB[a] h/r %free	Major elimination pathway[b]	Contr. 3A4[c]. (%)	OATP-1B1 inhib[d] IC_{50} μM	PK[e] rat/dog (*iv*)			
					CL mL/min/kg	t1/2 (h)	Vss (L/Kg)	F%
10	0.6/<0.04	Hydrox.	66	1.4	1.2/2.0	4.7/7.0	0.18/0.4	12/65
11	3.1/1.4	Red+gluc.	68	2.5	10/2.5	2.9/6.8	1.3/1.3	14/65
12	5.3/2.4	Hydrox + gluc.	94	2.3	36/7.6	0.45/2.1	1.1/1.1	14/65

See Supporting Information for full details. [a]Plasma protein binding (human or rat). [b]Hydrox: CYP450 oxidation in the cyclohexyl ring. Red: Ketone reduction to corresponding alcohol. Gluc: Phase II glucuronidation. [c]Contribution of CYP3A4 to CYP450 mediated metabolism considering a panel of six CYP isoforms (CYP1A2, CYP2C8, CYP2C9, CYP2C19, CYP2D6 and CYP3A4). [d]Inhibition of pivastatin uptake to HEK293 cells transfected with human OATP1B1. [e]CL, $t_{1/2}$ and Vss derived from *i.v.* data, F% from *p.o.*; Doses: rat *i.v.* 1 μmol/kg for **10**, **12**; 2 μmol/kg for **11**; rat *p.o.* 2 μmol/kg for

10, 2.8 μmol/kg for **11**, 2.5 μmol/kg for **12**; dog *i.v.* 1 μmol/kg for **10**, 2 μmol/kg for **11** and **12**; dog *p.o.* 2 μmol/kg for **10** and **12**; 4.2 μmol/kg for **11**.

Preclinical safety evaluation

Cell toxicity was generally low in the series and no cell toxicity as measured in THP-1 cells, or mitochondrial impairment as measured in HepG2 cells was seen for **10** to **12** (IC_{50} values > 250 μM). Compound **11** and **12** (no data for compound **10**) demonstrated inhibition of hBSEP and hMrp2 transport proteins with IC_{50} values of 74 to 340 μM, respectively, indicating sufficient margins to predicted human C_{max}. No activity was observed in a human aryl hydrocarbon receptor assay or a phospholipidosis assay. Compounds **10** to **12** did not demonstrate any ion channel interference (hERG, hIKs, hIto, hNav1.5) (IC_{50} values > 33 μM). Compounds **11** and **12** were further evaluated against additional ion channels and demonstrated IC_{50} values > 32 μM for HCN4, hCav3.2 and hKv1.5 (see Supporting Information). The secondary pharmacology profiles and off-target promiscuity were evaluated using a panel of 83 targets for **10** and 190 targets for **11**, **12** (Cerep, France). The three compounds displayed low promiscuity with > 30-fold margins

to predicted therapeutic exposures except for the adenosine transporter where compound **11** and **12** demonstrated 16- and 12-fold margin, respectively. In addition, compounds in this series did not show any effects on the production of other eicosanoids, generated by the cyclooxygenases COX-1 and COX-2, and compounds **10** to **12** displayed greater than 100-fold selectivity.

Earlier experimental work with the previous lead compound **1** indicated that dog was the most sensitive pre-clinical species with respect to increases in heart rate. Thus, compounds **10** to **12** were assessed in anaesthetized beagle dogs for their effects on heart rate, arterial blood pressure, electrocardiography and contractility parameters. To our disappointment, compound **10** was found to cause a rapid increase in heart rate and in left ventricular DP/dtmax (index of cardiac contractility) during the second infusion period (see Supporting Information for study details). Compounds **11** and **12** did not show any pronounced increase in heart rate or effect on contractility parameters at the doses tested and these compounds were therefore evaluated further in conscious dogs. Compound **11** was found to be poorly tolerated as adverse clinical signs, but not

cardiovascular related, were observed including repeated vomiting. Compound **12**, was well tolerated and no adverse clinical signs were observed. The effects of **12** on heart rate, arterial blood pressure, left ventricular parameters, lead II electrocardiogram and body temperature were assessed in conscious telemetered dogs, following single intravenous infusions at three dose levels. Intravenous infusion was used to attain a target plasma concentration 100-fold above predicted free C_{max} in humans at the predicted therapeutic dose. We were delighted that compound **12** did not produce any effects on the cardiovascular parameters assessed even at the highest achieved exposure (110-fold to predicted human free C_{max}). No treatment related cardiovascular findings (function or histopathology changes) were observed in the toxicology studies in rat and dog with up to 28-day duration of treatment.

Pre-clinical *in vivo* PK/PD relationship

With the promising safety profile and no adverse cardiovascular effects observed in dogs for compound **12**, we further investigated its ability to inhibit 5-LO pathway activity when dosed *in vivo*. The compounds in this series showed no inhibition of 5-LO

pathway activity in rodent blood but potently inhibited LTB_4 production in dog blood and hence dogs were utilized for preclinical PK/PD assessment.[26] Pharmacodynamic actions of **12** were initially assessed by measuring *ex vivo* LTB_4 production in whole blood. Full data sets and individual data are provided in the Supporting Information. Following administration of a single per oral (p.o.) dose (0.9 mg/kg, n=2, Study A), **12** suppressed LTB_4 production by > 90% with maximum inhibition reached within 2.5 h of administration. In a second study (B), **12** was administered as two p.o. doses separated by 48 h (day 1: 0.18 mg/kg, day 3: 0.09 mg/kg, n=2) and a greater than 90% reduction in LTB_4 production was observed after each dose, with the maximum effect occurring between 4 and 9 h after dosing. LTB_4 production returned towards baseline prior to the second dose, and reached baseline again 48 h after this dose, indicating reversibility of FLAP inhibition. In a third study, repeated once daily p.o. administration of **12** at 0.02, 0.09 and 0.2 mg/kg for 3 consecutive days (n=3 per dose; Study C, Figure 3) caused a concentration dependent inhibition of LTB_4 production throughout the dosing period that returned to baseline 24 h after the final dose.

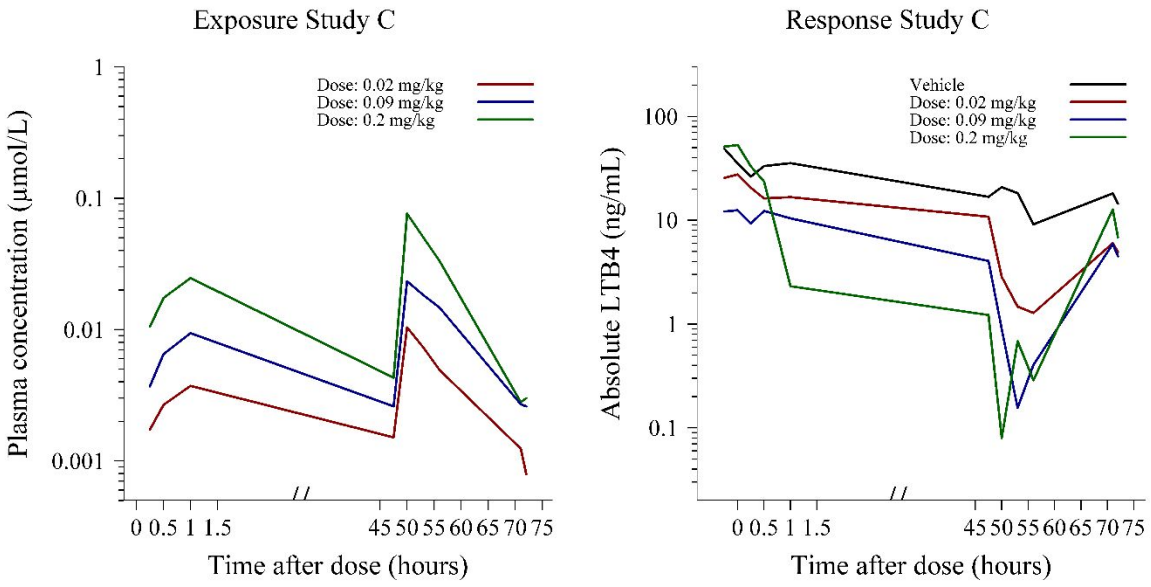

Figure 3. Median plasma concentrations of **12** and LTB_4 response after repeated once daily p.o. administration of **12** at 0.02, 0.09 and 0.2 mg/kg for 3 consecutive days, n=3 per dose; green 0.02 mg/kg, blue 0.09 mg/kg, red 0.2 mg/kg; n=3 per dose. No error margins given, see Supporting Information for full data set.

In order to also evaluate the effect of **12** on cysteinyl leukotriene production, endogenous LTE_4 levels in urine ($uLTE_4$) were measured at baseline and during the final 24 h in Study C. $uLTE_4$ levels were undetectable at the two highest doses, and suppressed by around 60% at the lowest dose, confirming that **12** also suppresses cysteinyl leukotriene production (Figure 4).

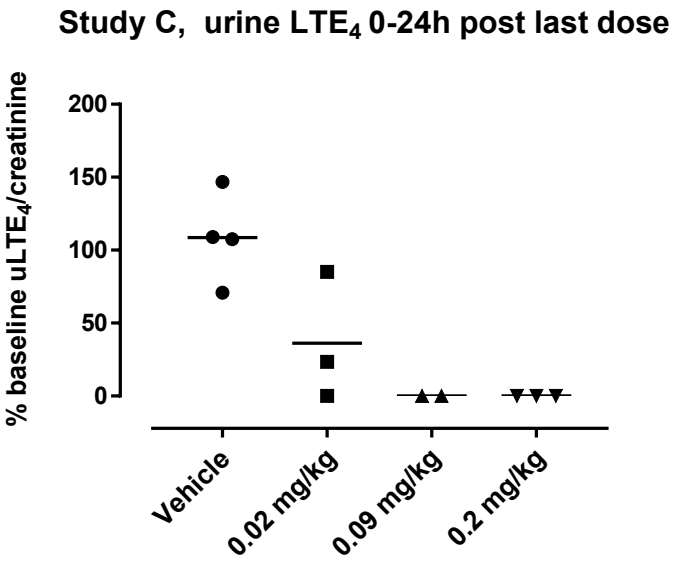

Figure 4. Inhibition of urinary LTE_4 ($uLTE_4$) levels (Study C) after administration with compound **12**. One dog in the medium dose group displayed $uLTE_4$ below LOQ at baseline and is excluded from the analysis.

To compare *in vitro* and *ex vivo* potency for **12** in dog whole blood, concentration response curves were generated for the *ex vivo* assays by plotting exposure against the baseline corrected LTB_4 level observed (Figure 5). Surprisingly, this analysis revealed

that the *ex vivo* potency of **12** was approximately 10-fold greater than the *in vitro* potency. The reason for this finding is not yet known but is under investigation.

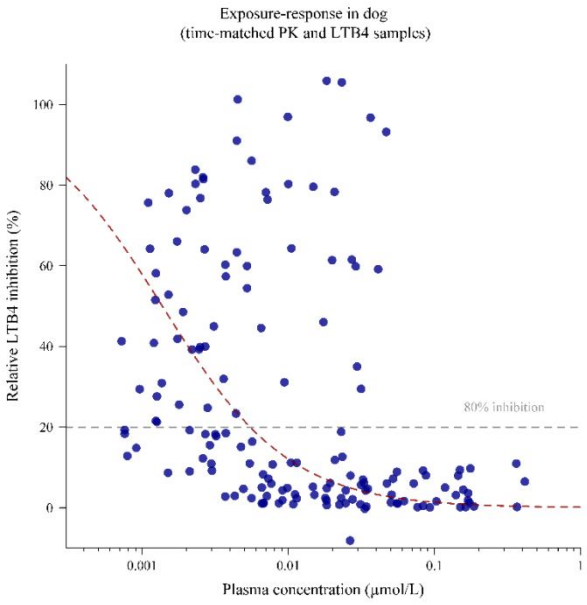

Figure 5. Exposure of **12** and LTB_4 response data from Studies A-C. (●) individual observations (---) estimated IC_{50}-curve.

With the highly improved cardiovascular safety profile, Ames negative amino-pyrazole ring and with an overall profile meeting our criteria for a clinical candidate, including potency and ADME properties suitable for oral dosing and no major safety concerns in the 28-day pre-clinical dog and rat toxicity studies, compound **12** was selected as the clinical candidate (AZD5718). After completion of the pre-clinical safety package for first

time in man studies, compound **12** entered Phase 1 clinical trials in 2016 and is currently (end 2018) in a Phase 2a trial for the treatment of Coronary Artery Disease.

Dose prediction for First Time In Man studies.

A target level of LTB_4 inhibition of 80% over 24 h was selected based on clinical data for the 5-LO inhibitor VIA-2291 indicating that this level of LTB_4 inhibition could translate into beneficial effects LVEF.[4, 5] Therefore, dose prediction for first time in man studies aimed for a dose of AZD5718 that would give at least this level of LTB_4-inhibition during the dosing interval. The dose was defined based on scaling of PK parameters from *in vitro* or *in vivo*, to predict the human exposure. The human clearance was scaled from human hepatocyte data using regression methods and the human volume of distribution at steady-state (Vss) was predicted based on the Oie-Tozer method.[27] The potency of AZD5718 was determined *in vitro* and from the exposure-response data generated in dog blood *ex vivo* as well as *in vitro* in a human whole blood assay. A PK/PD model was then developed based on these data and used to simulate different dose levels and dosing scenarios for AZD5718 in man. As hysteresis (time delay in response) was

observed in the exposure-response relationship in dog, an effect-compartment model was applied to describe the time-lag between AZD5718 exposure and LTB_4 effect.[28] This developed model could describe the time course and extent of LTB_4 inhibition.

The LTB_4 IC_{50}-value for AZD5718 was 39 nM and the IC_{80} value was 116 nM in the human whole blood assay, with the latter defining the minimum inhibitory concentration that would be needed during a dosing interval. The PK simulations predicted that, should our model be valid, a twice-daily dose of 65 mg (given as an immediate release formulation) of AZD5718 might achieve an exposure level above the defined minimum inhibitory concentration of 116 nM (IC_{80}) during the dosing interval. This dose prediction was in line with the early dose prediction (eD2M) presented in Table 1 (44 mg/day). However, the eD2M prediction does not take the PK profile into account and given the short, predicted human half-life of about the 3 h, a twice-daily dosing regimen was thought necessary to achieve sufficient LTB_4 inhibition throughout the day.

Human studies of AZD5718 in healthy subjects

AZD5718 was administered in a single ascending dose (SAD) and multiple ascending dose (MAD) study as an oral suspension. In the SAD study, AZD5718 was administered in single doses of 25, 50, 100, 300, 600 and 1200 mg ((NCT02632526).[28] In the MAD study, healthy subjects were given once daily doses of 60, 180, 300 and 600 mg for 10 days (Figure 6). Following administration of an oral suspension of AZD5718, the compound was rapidly absorbed and maximum plasma concentration (Cmax) was generally reached within 1 to 2 h. A more than dose proportional increase in both area under the curve (AUC) and C_{max} was observed in the explored dose range, whereas C_{trough} concentrations appeared to increase dose proportionally. In agreement with an observed half-life of approximately 12 h, steady-state levels were achieved after 2 to 3 days following once daily dosing and the steady-state exposure was approximately 30% to 40% higher compared to SAD data. The observed half-life in man was longer than predicted based on our pre-clinical data (3 h predicted versus 12 h observed), and this was likely driven by a larger volume of distribution than expected when scaling from rat and dog.

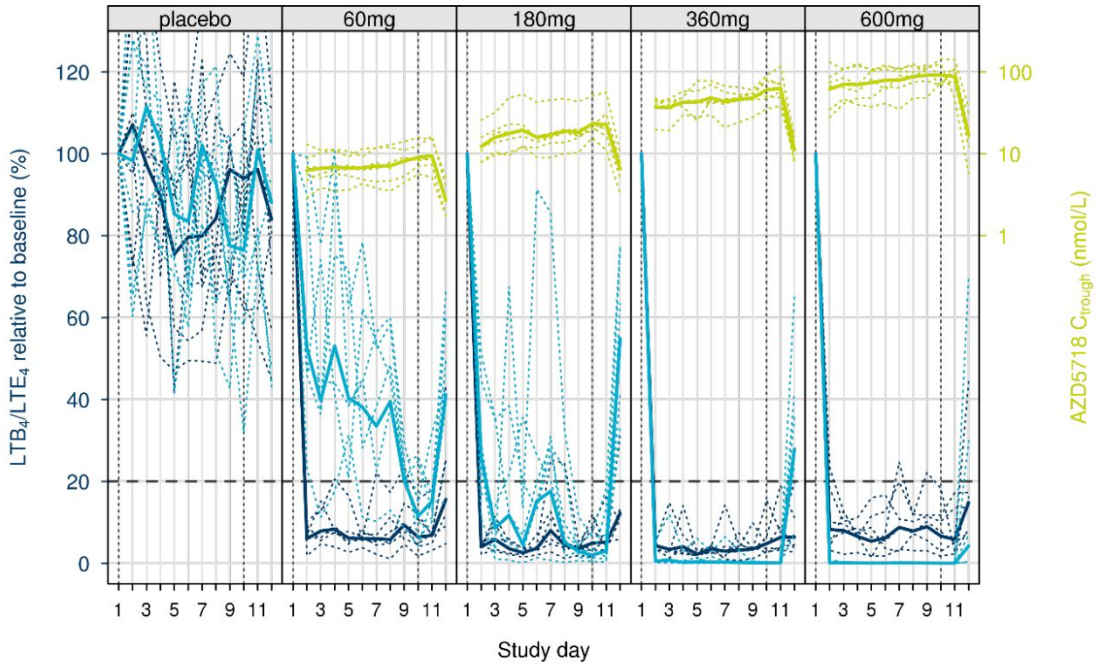

Figure 6. Plasma LTB_4 (light blue) and urine LTE_4 (dark blue) relative to baseline at AZD5718 C_{trough} following oral daily dosing of AZD5718 to healthy volunteers at doses of 60, 180, 300 and 600 mg for 10 days (study NCT02632526). Solid lines represent median and dotted lines individual subjects.

Dose dependent target engagement, as assessed by measuring *ex vivo* calcium ionophore stimulated LTB_4 production in fresh blood and endogenous LTE_4 levels in urine, was observed after both single and repeated dosing of AZD5718 for 10 days (Figure 6). As shown in Figure 7, a clear plasma concentration-effect relationship was

seen for both LTB_4 and LTE_4. Visual inspection of the data suggest a C_{trough} value > 15 nM will achieve reduction of the plasma LTB_4 levels by > 80% over 24 h, i.e. the predicted level of inhibition is achieved at ~8-fold lower concentrations compared to *in vitro* data. The reason for this discrepancy in potency is not known but mirrors the observations seen previously in the dog ($IC_{50free\ (in\ vitro\ dog)}$: 1.0 nM versus $IC_{50free\ (ex\ vivo\ dog)}$: 0.1 nM).

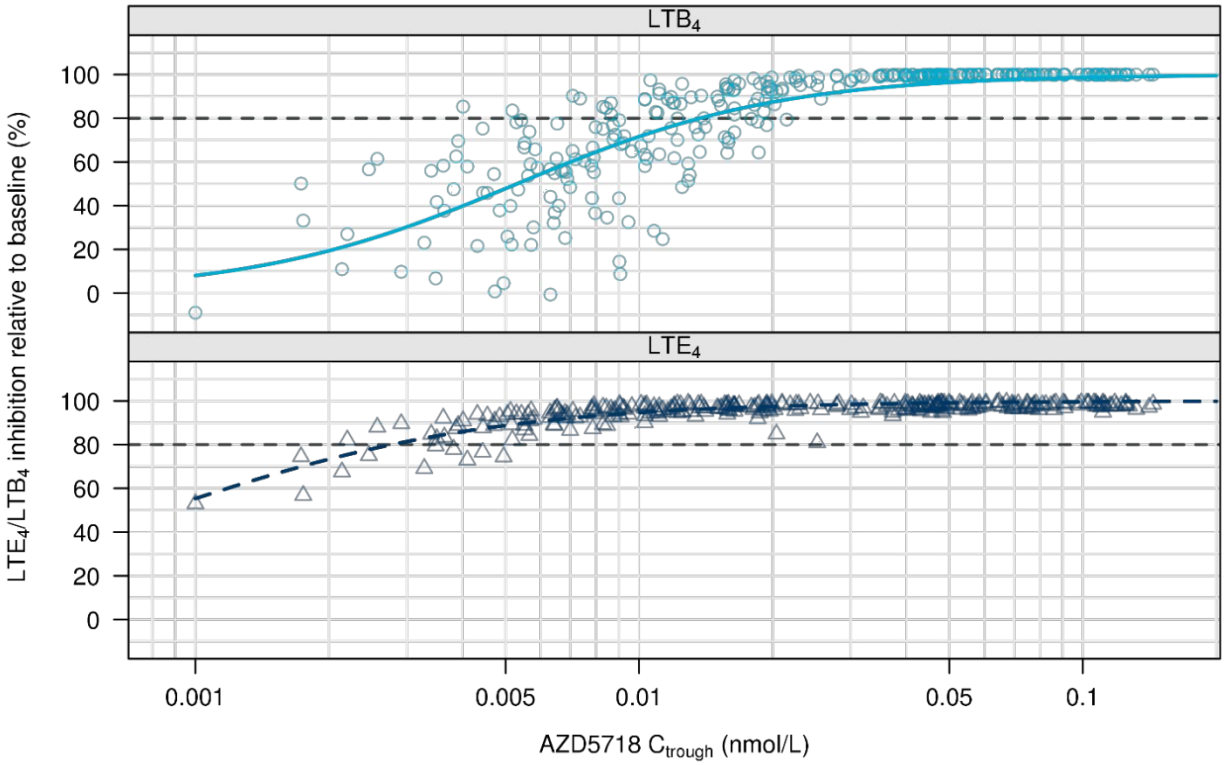

Figure 7. Relative LTB_4/LTE_4 inhibition at AZD5718 C_{trough} in study NCT02632526. The solid line shows the fit of the data to a simple E_{max} model.

The PK parameters of AZD5718 in combination with the sustained effect on the target engagement biomarkers LTB_4 and LTE_4 throughout 24 h supported future once daily dosing, provided that a similar PK and PK/PD relationship is observed in patients as that seen in healthy subjects.

The effect of AZD5718 on LTB_4 inhibition was of a similar magnitude as that reported for the 5-LO inhibitor VIA2291, while inhibition of LTE_4 production was much more pronounced and seen at lower concentrations compared to VIA2291.[4] This finding is in agreement with observations for another FLAP inhibitor, AM103, which showed a more pronounced effect on endogenous LTE_4 production at lower concentrations compared to the effect seen on LTB_4 although the concentrations needed to achieve this inhibition was much higher than that for AZD5718.[29] The AZD5718 IC_{50} value for the effect on *ex vivo* stimulated LTB_4 inhibition in human blood samples is almost 100-fold lower compared to both AM103 and VIA2291. It is noteworthy that 6 months once daily treatment with VIA2291 resulted in similar LTB_4 inhibition as was seen for AZD5718 in the present study

and was associated with a beneficial effect on plaque progression and a dose-dependent improvement in LVEF in acute coronary syndrome (ACS) patients.

Conclusion

Herein we have highlighted the medicinal chemistry story behind the identification and discovery of the clinical FLAP inhibitor AZD5718 (**12**). Key drivers for the compound design included securing metabolic stability, PK properties and potency in human whole blood compatible with oral dosing leading to clinically relevant exposures. The finding of the Ames negative bicyclic amino-pyrazole ring as a key motif in AZD5718 and the much-improved cardiovascular safety profile for AZD5718 compared to earlier frontrunner compounds were critical for the selection of AZD5718. Pre-clinical toxicology studies in rat and dog did not show any serious adverse events of clinical significance and thus AZD5718 entered Phase 1 trials in healthy volunteers in 2016. The safety and tolerability results in humans showed no serious adverse events (SAEs) or drug related adverse events (AEs) of clinical significance, at the doses tested. These observations, together with the PK and PD response on target biomarkers, supported continued clinical development of AZD5718 in patients. The clinical relevance of the higher LTB_4 inhibitory potency of AZD5718 relative to VIA2291 and its more pronounced effect on the LTE_4 pathway is currently investigated in patients with coronary artery disease (NCT03317002).

EXPERIMENTAL SECTION

General synthesis details including ^{1}HNMR spectra and synthesis information for compounds **1**-**12** are described in the Supporting Information. Below are specified synthesis for key compounds **10**, **11** and **12** (AZD5718). All tested FLAP inhibitors **1**-**12** have purity >95% (LCMS/UV, see supporting information for details; compound **9** displayed 89% purity, further purification proved difficult).

***N*-*tert*-butoxy-1-methyl-4-({(1*R*,2*R*)-2-[4-(5-methyl-1*H*-pyrazol-3-yl)benzoyl]cyclohexane-1-carbonyl}amino)-1*H*-pyrazole-5-carboxamide (10)**

Methyl 4-{[(1R,2R)-2-(4-bromobenzoyl)cyclohexane-1-carbonyl]amino}-1-methyl-1H-pyrazole-5-carboxylate: Triethylamine (20 mL, 144 mmol) and T3P (50% in EtOAc, 42 mL, 71 mmol) were added to a solution of (1*R*,2*R*)-2-(4-bromobenzoyl)cyclohexanecarboxylic acid (10.87 g, 34.93 mmol) and methyl 4-amino-1-methyl-1*H*-pyrazole-5-carboxylate (10.0 g, 64.5 mmol) in EtOAc (130 mL) and the reaction mixture was heated to 73 °C and stirred at that temperature for 2 h and at 40

°C for 1 h. The reaction mixture was cooled to rt and the mixture was diluted with EtOAc and extracted with saturated aqueous $NaHCO_3$(aq). The organic phase was dried (phase separator) and the solvent was removed under reduced pressure to give crude methyl 4-{[(1*R*,2*R*)-2-(4-bromobenzoyl)cyclohexane-1-carbonyl]amino}-1-methyl-1*H*-pyrazole-5-carboxylate (14 g, 87%); ^{1}H NMR (400 MHz, $CDCl_3$) δ 8.87 (s, 1H), 8.10 (s, 1H), 7.79 – 7.87 (m, 2H), 7.52 – 7.59 (m, 2H), 4.05 (s, 3H), 4.00 (s, 3H), 3.60 – 3.72 (m, 1H), 2.92 (s, 1H), 1.96 – 2.14 (m, 2H), 1.80 – 1.95 (m, 2H), 1.61 – 1.75 (m, 1H), 1.27 – 1.53 (m, 3H); MS m/z 448.4 $[M + H]^+$. The material was taken to the next step without further purifications.

4-{[(1R,2R)-2-(4-Bromobenzoyl)cyclohexane-1-carbonyl]amino}-1-methyl-1H-pyrazole-5-carboxylic acid: A solution of crude methyl 4-{[(1*R*,2*R*)-2-(4-bromobenzoyl)cyclohexane-1-carbonyl]amino}-1-methyl-1*H*-pyrazole-5-carboxylate (12.7 g, 28.33 mmol) in THF (40 mL), MeOH (40 mL) and aqueous LiOH (1M, 40 mL, 40 mmol) was added and stirred at rt for 2.5 h. More aqueous LiOH (1M, 15 mL, 15 mmol) was added and the reaction was stirred for 90 min. Additional aqueous LiOH (1M, 5 mL, 5 mmol) was added and the reaction mixture was concentrated. Saturated NaCl(aq)

EtOAc were added to the residue and the pH was adjusted to ~2 using aqueous HCl (3.8 M). The phases were separated and the organic phase was dried through a phase-separator. The solvent was removed from the organic phase under reduced pressure to give 4-{[(1*R*,2*R*)-2-(4-bromobenzoyl)cyclohexane-1-carbonyl]amino}-1-methyl-1*H*-pyrazole-5-carboxylic acid (12.3 g, ~100%) as white solid; MS m/z 432.2 $[M – H]^-$. The material was taken to the next step without further purifications.

4-{[(1R,2R)-2-(4-Bromobenzoyl)cyclohexane-1-carbonyl]amino}-N-tert-butoxy-1-methyl-1H-pyrazole-5-carboxamide: HATU (6.6 g, 17.36 mmol) and DIPEA (5.69 mL, 32.60 mmol) were added to a solution of crude 4-{[(1*R*,2*R*)-2-(4-bromobenzoyl)cyclohexane-1-carbonyl]amino}-1-methyl-1*H*-pyrazole-5-carboxylic acid (6.436 g, 14.82 mmol) in DMF (60 mL). After 1-2 minutes *O*-(*tert*-butyl)hydroxylamine hydrochloride (3.72 g, 29.64 mmol) was added and the reaction mixture was stirred at rt for 5 h. The mixture was quenched by adding saturated $NaHCO_3$(aq) and EtOAc. The phases were separated then the organic phase was washed with saturated $NaHCO_3$(aq), saturated NH_4Cl(aq) and finally saturated NaCl(aq) before drying the organic phase

through a phase-separator. The solvents were evaporated leaving to give 4-{[(1*R*,2*R*)-2-(4-bromobenzoyl)cyclohexane-1-carbonyl]amino}-*N*-*tert*-butoxy-1-methyl-1*H*-pyrazole-5-carboxamide (7.6 g, ~100%) as an off-white solid; ^{1}H NMR (400 MHz, $CDCl_3$) δ 9.22 (br s, 1H), 8.07 (br s, 1H), 7.79 – 7.85 (m, 2H), 7.57 – 7.63 (m, 3H), 4.01 (s, 3H), 3.57 – 3.69 (m, 1H), 2.80 – 2.88 (m, 1H), 1.99 – 2.15 (m, 2H), 1.82 – 1.96 (m, 2H), 1.60 – 1.76 (m, 1H), 1.33 – 1.54 (m, 3H), 1.30 (s, 9H); MS m/z 505.3 $[M + H]^+$. The product was pure enough for further synthesis.

N-tert-butoxy-1-methyl-4-{[(1R,2R)-2-{4-[3-methyl-1-(oxan-2-yl)-1H-pyrazol-5-yl]benzoyl}cyclohexane-1-carbonyl]amino}-1H-pyrazole-5-carboxamide: To 4-{[(1*R*,2*R*)-2-(4-bromobenzoyl)cyclohexane-1-carbonyl]amino}-*N*-*tert*-butoxy-1-methyl-1*H*-pyrazole-5-carboxamide (9 g, 17.81 mmol) was added a solution of 3-methyl-1-(oxan-2-yl)-5-(4,4,5,5-tetramethyl-1,3,2-dioxaborolan-2-yl)-1*H*-pyrazole (11.2 g, 29.5 mmol) in dioxane (100 mL). Then, a solution of K_2CO_3 (9.84 g, 71.2 mmol) in water (100 mL) was added and the resulting solution was evacuated and back-filled with N_2 three times. The reaction mixture was heated to ca 55°C, Pd(dtbpf)Cl_2 (0.607 g, 0.94 mmol) was added and the

reaction mixture was heated to 80°C for 30 min. The reaction mixture was then cooled to rt, diluted with EtOAc and washed with saturated NaCl(aq). The organic phase was dried (phase separator) and concentrated in vacuo. The residue was purified by flash chromatography (50%→100% EtOAc in heptane) to give *N-tert*-butoxy-1-methyl-4-{[(1*R*,2*R*)-2-{4-[3-methyl-1-(oxan-2-yl)-1*H*-pyrazol-5-yl]benzoyl}cyclohexane-1-carbonyl]amino}-1*H*-pyrazole-5-carboxamide (8 g, 76%); MS m/z 589.5 $[M – H]^-$.

N-tert-butoxy-1-methyl-4-({(1R,2R)-2-[4-(5-methyl-1H-pyrazol-3-yl)benzoyl]cyclohexane-1-carbonyl}amino)-1H-pyrazole-5-carboxamide (**10**):

Aqueous HCl (3.8 M, 10 mL, 38 mmol) was added to a solution of *N-tert*-butoxy-1-methyl-4-{[(1*R*,2*R*)-2-{4-[3-methyl-1-(oxan-2-yl)-1*H*-pyrazol-5-yl]benzoyl}cyclohexane-1-carbonyl]amino}-1*H*-pyrazole-5-carboxamide (11.4 g, 19.30 mmol) in dioxane (100 mL) and H2O (50 mL) at 5 °C and the reaction mixture was allowed to reach 17 °C over 1 h 40 min. The reaction mixture was cooled to 5 °C and more aqueous HCl (3.8 M, 3 mL, 11 mmol) was added and the reaction mixture was allowed to reach 17 °C over 2 h. The reaction mixture was then diluted with EtOAc and the organic phase was washed with

saturated $NaHCO_3$(aq). The aqueous phase was extracted with EtOAc (x2) and the combined organic phase was washed with saturated NaCl(aq), dried (phase-separator) and evaporated. The residue was purified by flash chromatography (EtOAc) to give 10 (8.50 g, 87%); ^{1}H NMR (400 MHz, DMSO-d6) δ 12.74 (s, 1H), 10.70 (s, 1H), 9.48 (s, 1H), 7.96 – 8.05 (m, 2H), 7.82 – 7.93 (m, 2H), 7.45 (s, 1H), 6.55 (s, 1H), 3.85 (s, 3H), 3.65 – 3.77 (m, 1H), 2.80 – 2.94 (m, 1H), 2.28 (s, 3H), 2.01 – 2.12 (m, 1H), 1.96 (d, *J* = 11.3 Hz, 1H), 1.79 (dd, *J* = 28.9, 12.3 Hz, 2H), 1.41 – 1.58 (m, 2H), 1.26 – 1.4 (m, 2H), 1.20 (s, 9H); HRMS (ESI) m/z calcd for $C_{27}H_{35}N_6O_4$ $[M + H]^+$ 507.2714; found 507.2709.

(1*R*,2*R*)-2-[4-(3-Methyl-1H-pyrazol-5-yl)benzoyl]-*N*-(1-methyl-5-sulfamoyl-1H-pyrazol-4-yl)cyclohexanecarboxamide (11)

Ethyl 5-(benzylsulfanyl)-1-methyl-1H-pyrazole-4-carboxylate: Dibenzyl disulfide (101.9 g, 413.57 mmol) was added in portions to a solution of ethyl 5-amino-1-methyl-1*H*-pyrazole-4-carboxylate (10 g, 59.11 mmol) in ACN (400 mL) in an atmosphere of nitrogen and at rt. CuCl (293 mg, 7.14 mmol) was added in portions at rt to the reaction mixture and it was stirred at rt for 30 min. 3-Methyl-1-nitrobutane (41.5 g, 354.26 mmol) was added to

the reaction mixture and the resulting solution was stirred at rt for 30 min and then at 60°C for 1 h. The reaction mixture was allowed to reach rt and the solids were filtered off. The filtrate was concentrated under vacuum and the residue was purified by silica gel column chromatography (EtOAc/petroleum ether, 1:8) to give Ethyl 5-(benzylsulfanyl)-1-methyl-1H-pyrazole-4-carboxylate (11.6 g, 71%) as yellow oil. MS *m/z* 277 $[M+H]^+$.

5-(Benzylsulfanyl)-1-methyl-1H-pyrazole-4-carboxylic acid: Sodium hydroxide (5.04 g, 126.01 mmol) in water (30 mL) was added dropwise at 0°C to a solution of ethyl 5-(benzylsulfanyl)-1-methyl-1*H*-pyrazole-4-carboxylate (11.6 g, 41.98 mmol) in MeOH (150 mL) and the reaction mixture was stirred at rt for 15 h. The reaction mixture was concentrated under vacuum, the residue was dissolved in water and the aqueous phase was washed EtOAc. The pH of the aqueous layer was adjusted to 5~6 with HCl (12 M, aq) and the solids formed were collected by filtration and dried under vacuum to give 5-(Benzylsulfanyl)-1-methyl-1H-pyrazole-4-carboxylic acid (8.8 g, 84%) as a light yellow solid. MS *m/z* 249 $[M+H]^+$.

tert-Butyl [5-(benzylsulfanyl)-1-methyl-1H-pyrazol-4-yl]carbamate: Boc_2O (30 g, 137.61 mmol) and Et_3N (10.7 g, 105.74 mmol) was added under an atmosphere of nitrogen to a solution of 5-(benzylsulfanyl)-1-methyl-1*H*-pyrazole-4-carboxylic acid (8.8 g, 35.44 mmol) in *tert*-butanol (200 mL). Diphenyl phosphoryl azide (19.5 g, 70.86 mmol) was added dropwise to the reaction mixture and it was stirred at rt for 4 h and then at 88°C for 15 h. The reaction mixture was concentrated under vacuum. The residue was dissolved in EtOAc and the organic phase was washed with $NaHCO_3$ (sat, aq) and brine, dried over Na_2SO_4, filtered and concentrated under vacuum. The residue was purified by silica gel column chromatography (EtOAc/petroleum ether, 1:6) to give tert-Butyl [5-(benzylsulfanyl)-1-methyl-1H-pyrazol-4-yl]carbamate (9.8 g, 87%) as yellow oil. MS *m/z* 320 $[M+H]^+$.

5-(Benzylsulfanyl)-1-methyl-1H-pyrazol-4-amine hydrochloride: HCl (g) was bubbled into a solution of *tert*-butyl [5-(benzylsulfanyl)-1-methyl-1*H*-pyrazol-4-yl]carbamate (9.8 g, 30.68 mmol) in MeOH (150 mL) at rt for 6 h. The reaction mixture was concentrated under vacuum to give 5-(Benzylsulfanyl)-1-methyl-1H-pyrazol-4-amine hydrochloride (7.5 g,

96%) as a solid. ^{1}H NMR (400 MHz, DMSO-d6) δ 10.61 (br s, 2H), 7.66 (s, 1H), 7.24 – 7.31 (m, 3H), 7.14 – 7.21 (m, 2H), 4.20 (s, 3H), 3.25 (s, 2H); MS *m/z* 220 $[M+H]^+$.

(1R,2R)-N-[5-(Benzylsulfanyl)-1-methyl-1H-pyrazol-4-yl]-2-(4-bromobenzoyl)cyclohexanecarboxamide: To a slurry of (1*R*,2*R*)-2-[(4-bromophenyl)carbonyl]cyclohexane-1-carboxylic acid (2.7 g, 8.68 mmol), 5-(benzylsulfanyl)-1-methyl-1*H*-pyrazol-4-amine hydrochloride (2.91 g, 9.54 mmol) and pyridine (4 mL, 49.46 mmol) in ethyl acetate (26 mL) was added T3P (50% in ethyl acetate) (13 mL, 21.84 mmol) at 0°C during 1h. The reaction was allowed to warm to room temperature overnight. The reaction mixture was diluted with ethyl acetate, cooled to 0°C and was washed with 0.7M HCl, $NaHCO_3$ (sat, aq) and brine, dried, filtered and concentrated under vacuum to give (1*R*,2*R*)-N-[5-(Benzylsulfanyl)-1-methyl-1H-pyrazol-4-yl]-2-(4-bromobenzoyl)cyclohexanecarboxamide (4.2 g, 94%) as a solid. ^{1}H NMR (400 MHz, CDCl3) δ 7.95 (s, 1H), 7.83 (d, *J* = 8.6 Hz, 2H), 7.58 (d, *J* = 8.6 Hz, 2H), 7.22 – 7.32 (m, 3H), 7.14 (s, 1H), 6.96 – 7.03 (m, 2H), 3.76 (s, 2H), 3.61 – 3.71 (m, 1H), 3.43 (s, 3H), 2.71 – 2.82 (m, 1H), 1.83 – 2.09 (m, 4H), 1.64 – 1.78 (m, 1H), 1.25 – 1.56 (m, 3H); MS m/z 512 $[M+H]^+$.

(1R,2R)-2-(4-Bromobenzoyl)-N-(1-methyl-5-sulfamoyl-1H-pyrazol-4-yl)cyclohexanecarboxamide: Stage 1. A mixture of (1*R*,2*R*)-*N*-[5-(benzylsulfanyl)-1-methyl-1*H*-pyrazol-4-yl]-2-(4-bromobenzoyl)cyclohexanecarboxamide (7 g, 13.66 mmol)

in AcOH (60 mL) was diluted with water and cooled to -10°C. 1,3-Dichloro-5,5-dimethylimidazolidine-2,4-dione (4.05 g, 20.56 mmol) was added in one portion at -10°C and the reaction mixture was stirred at -5°C for 30 min. 1,3-Dichloro-5,5-dimethylimidazolidine-2,4-dione (1.35 g, 6.85 mmol) was added at 0°C and the reaction mixture was stirred for 30 min. 1,3-Dichloro-5,5-dimethytlimidazolidine-2,4-dione (1.35 g, 6.85 mmol) was added at about -5°C and the reaction mixture was stirred for 30 min. 1,3-Dichloro-5,5-dimethylimidazolidine-2,4-dione (1.35 g, 6.85 mmol) was added at about -5°C and the reaction mixture was stirred below 5°C for 60 min. The reaction mixture was diluted with water and the aqueous phase was extracted with DCM. The organic layer was washed with $NaHCO_3$ (8%, aq) until pH of the aqueous layer was about 6~7. The organic phase was concentrated under vacuum to give 4-({[(1*R*,2*R*)-2-(4-bromobenzoyl)cyclohexyl]carbonyl}amino)-1-methyl-1*H*-pyrazole-5-sulfonyl chloride (12 g, crude). MS 488 *m/z* $[M+H]^+$. *Stage 2.* NH_3 (g) was bubbled into THF (300 mL) at -5°C until the solvent was near saturation. A solution of 4-({[(1*R*,2*R*)-2-(4-bromobenzoyl)cyclohexyl]carbonyl}amino)-1-methyl-1*H*-pyrazole-5-sulfonyl chloride (19 g, 38.87 mmol) in THF (500 mL) was added dropwise with stirring at -5°C and the reaction

mixture was stirred at rt for 30 min. The reaction mixture was concentrated under vacuum and the residue was purified by silica gel column chromatography (EtOAc/petroleum ether, 1:1) and then by silica gel medium pressure column chromatography using a gradient of 20%-45% of ACN in H_2O/HCO_2H (99.9/0.1) buffer system as mobile phase to give (1*R*,2*R*)-2-(4-Bromobenzoyl)-N-(1-methyl-5-sulfamoyl-1H-pyrazol-4-yl)cyclohexanecarboxamide. (12.0 g, 66%) as a solid. MS 469 *m/z* $[M+H]^{+.}$

*(1R,2R)-2-[4-(3-Methyl-1H-pyrazol-5-yl)benzoyl]-N-(1-methyl-5-sulfamoyl-1H-pyrazol-4-yl)cyclohexanecarboxamide (*11*):*

$PdCl_2$(dppf)-DCM (4.87 g, 5.97 mmol) was added to a mixture of (1*R*,2*R*)-2-(4-bromobenzoyl)-*N*-(1-methyl-5-sulfamoyl-1*H*-pyrazol-4-yl)cyclohexanecarboxamide (28 g, 59.7 mmol), (5-methyl-1*H*-pyrazol-3-yl)boronic acid (15.02 g, 119.31 mmol) and sodium carbonate (25.3 g, 238.63 mmol) in dioxane (500 mL) and water (125 mL) under nitrogen atmosphere and the reaction mixture was stirred at 85°C for 4 h. The reaction mixture was concentrated under vacuum and diluted with EtOAc and the organic phase was washed with brine (sat., aq), dried over Na_2SO_4, filtered and evaporated. The crude

product was purified by Flash column chromatography on a C18 column (32μm, 400g), using a gradient from 0→40% of ACN in water as mobile phase to give the title compound (12.73 g, 45.3 %) as a solid; ^{1}H NMR (600 MHz, DMSO-d6) δ 12.98 (s, 1H), 9.05 (s, 1H), 8.24 (d, *J* = 8.1 Hz, 4H), 8.12 (d, J = 7.8 Hz, 2H), 8.03 (s, 1H), 6.79 (s, 1H), 4.18 (s, 3H), 3.88 – 4 (m, 1H), 3.05 – 3.14 (m, 1H), 2.50 (s, 3H), 2.24 – 2.32 (m, 1H), 2.16 – 2.23 (m, 1H), 2.02 – 2.11 (m, 1H), 1.93 – 2.02 (m, 1H), 1.66 – 1.78 (m, 2H), 1.54 – 1.65 (m, 1H), 1.34 – 1.45 (m, 1H); HRMS (ESI) m/z calcd for $C_{22}H_{27}N_6O_4S$ $[M + H]^+$ 471.1809, found 471.1808.

(1*R*,2*R*)-2-{4-[3-Methyl-1-(tetrahydro-2*H*-pyran-2-yl)-1*H*-pyrazol-5-yl]benzoyl}-*N*-(4-oxo-4,5,6,7-tetrahydropyrazolo[1,5-*a*]pyrazin-3-yl)cyclohexanecarboxamide (12)

Methyl 4-[(tert-butoxycarbonyl)amino]-1H-pyrazole-5-carboxylate: Di-*tert*-Butyl dicarbonate (159 mL, 0.68 mol) was added to methyl 4-amino-1*H*-pyrazole-3-carboxylate (87.6 g, 0.62 mol) and pyridine (100 mL, 1.24 mol) in CH_3OH (1 L) at 10 °C over a period

of 15 min. The reaction mixture was stirred at rt for 5 h. The solvent was removed under vacuum. The crude product was purified by crystallization from CH_3OH (700 mL) to give methyl 4-[(*tert*-butoxycarbonyl)amino]-1*H*-pyrazole-5-carboxylate (80 g, 53 %) as a purple solid. ^{1}H NMR (400 MHz, CD_3OD) δ 7.99 (s, 1H), 3.92 (s, 3H), 1.53 (s, 9H); MS *m/z* 228 $[M+H]^+$.

Methyl 1-(2-bromoethyl)-4-[(tert-butoxycarbonyl)amino]-1H-pyrazole-5-carboxylate: 1,2-Dibromoethane (1.97 mL, 22.8 mmol) was added to a solution of methyl 4-[(*tert*-butoxycarbonyl)amino]-1*H*-pyrazole-5-carboxylate (5.0g, 20.7 mmol) and K_2CO_3 (4.3 g, 31.1 mmol) in DMF (50 mL) at 0 °C over a period of 10 min and the reaction mixture was stirred at rt for 5 h. Water was added to the reaction mixture and the aqueous phase was extracted with EtOAc. The organic layer was dried over $MgSO_4$, filtered and evaporated and the crude product was purified by flash column chromatography (5%→20% 2-methylpentane in EtOAc). Pure fractions were evaporated to dryness to give methyl 1-(2-bromoethyl)-4-[(*tert*-butoxycarbonyl) amino]-1*H*-pyrazole-5-carboxylate (2.5 g, 35 %) as

a colorless oil. ^{1}H NMR (300 MHz, DMSO-d_6) δ 8.24 (s, 1H), 7.86 (s, 1H), 4.79 (t, J = 6.3 Hz, 2H), 3.87 (s, 3H), 3.80 (t, J = 6.3 Hz, 2H), 1.47 (s, 9H); MS *m/z* 348 $[M+H]^+$.

Tert-butyl (4-oxo-4,5,6,7-tetrahydropyrazolo[1,5-a]pyrazin-3-yl)carbamate: Ammonia hydrate (10 g, 287.2 mmol) was added to a solution of methyl 1-(2-bromoethyl)-4-[(*tert*-butoxycarbonyl)amino]-1*H*-pyrazole-5-carboxylate (10.0 g, 28.7 mmol) in CH_3CN (100 mL) and the reaction vessel was sealed and heated at 90 ^oC for 20 h. The solvent was removed under vaccum and the crude product was purified by flash column chromatography (1%→10% DCM in CH_3OH). Pure fractions were evaporated to dryness to give *tert*-butyl (4-oxo-4,5,6,7-tetrahydropyrazolo[1,5-*a*]pyrazin-3-yl)carbamate (6.0 g, 83 %) as a white solid. ^{1}H NMR (400MHz, DMSO-d_6) δ 8.30 (s, 1H) 7.95 (s, 1H),. 7.76 (s, 1H), 4.22 (t, J = 6.0 Hz, 2H), 3.55-3.65 (m, 2H), 1.47 (s, 9H); MS *m/z* 253 $[M+H]^+$.

3-Amino-6,7-dihydropyrazolo[1,5-a]pyrazin-4(5H)-one hydrochloride: HCl(g) was added to a solution of tert-butyl (4-oxo-4,5,6,7-tetrahydropyrazolo[1,5-a]pyrazin-3-yl)carbamate (9 g, 35.68 mmol) in CH_3OH (50 mL) and the reaction mixture was stirred

at rt for 2 h. The precipitate was collected by filtration, washed with EtOAc and dried under vacuum to give 3-amino-6,7-dihydropyrazolo[1,5-*a*]pyrazin-4(5*H*)-one hydrochloride (6.00 g, 89 %) as a white solid. ^{1}H NMR (400MHz, DMSO-d_6) δ 10.10-9.10 (m, 2H), 8.51 (s, 1H), 7.65 (s, 1H), 4.33 (t, *J* = 6.2 Hz, 2H), 3.58-3.66 (m, 2H); MS *m/z* 153 $[M+H]^+$.

(1R,2R)-2-(4-Bromobenzoyl)-N-(4-oxo-4,5,6,7-tetrahydropyrazolo[1,5-a]pyrazin-3-yl)cyclohexanecarboxamide: A mixture of 3-amino-6,7-dihydropyrazolo[1,5-*a*]pyrazin-4(5*H*)-one hydrochloride (1.0 g, 5.30 mmol) and Et_3N (2.96 mL, 21.21 mmol) in DMF (10 mL) was added to a stirred solution of (1*R*,2*R*)-2-(4-bromobenzoyl)cyclohexanecarboxylic acid (1.82 g, 5.83 mmol) and HATU (4.03 g, 10.60 mmol) in DMF (10 mL), over a period of 5 min. The reaction mixture was stirred at 50 ^oC for 15 h. The reaction mixture was diluted with EtOAc, and washed sequentially with $NaHCO_3$ (sat, aq), brine (sat.), and water. The organic layer was dried over $MgSO_4$, filtered and evaporated and the crude product was purified by flash column chromatography (1%→10% DCM in CH_3OH). Pure fractions were evaporated to dryness to give (1*R*,2*R*)-2-(4-bromobenzoyl)-*N*-(4-oxo-4,5,6,7-tetrahydropyrazolo[1,5-*a*]pyrazin-3-yl)cyclohexanecarboxamide (1.2 g, 51 %) as

a white solid. ^{1}H NMR (500 MHz, $CDCl_3$) δ 8.78 (s, 1H), 8.12 (s, 1H), 7.83 – 7.88 (m, 2H), 7.57 – 7.61 (m, 2H), 5.99 (s, 1H), 4.27 – 4.34 (m, 2H), 3.74 – 3.79 (m, 2H), 3.68 (ddd, *J* = 12.6, 10.4, 3.4 Hz, 1H), 2.94 (ddd, *J* = 12.7, 10.4, 3.8 Hz, 1H), 2.11 – 2.17 (m, 1H), 1.98 – 2.06 (m, 1H), 1.81 – 1.93 (m, 2H), 1.55 – 1.71 (m, 1H), 1.35 – 1.5 (m, 2H), 1.25 – 1.34 (m, 1H); MS *m/z* 445 $[M+H]^+$.

(1R,2R)-2-{4-[3-Methyl-1-(tetrahydro-2H-pyran-2-yl)-1H-pyrazol-5-yl]benzoyl}-N-(4-oxo-4,5,6,7-tetrahydropyrazolo[1,5-a]pyrazin-3-yl)cyclohexanecarboxamide:

Pd(dppf)Cl_2·DCM (0.092 g, 0.11 mmol) was added to a solution of (1*R*,2*R*)-2-(4-bromobenzoyl)-*N*-(4-oxo-4,5,6,7-tetrahydropyrazolo[1,5-*a*]pyrazin-3-yl)cyclohexanecarboxamide (1.0 g, 2.25 mmol), 3-methyl-1-(tetrahydro-2*H*-pyran-2-yl)-5-(4,4,5,5-tetramethyl-1,3,2-dioxaborolan-2-yl)-1*H*-pyrazole[30] (0.984 g, 3.37 mmol) and Na_2CO_3 (0.952 g, 8.98 mmol) in dioxane (20 mL) and water (5 mL) over a period of 10 min under nitrogen atmosphere. The reaction mixture was stirred at 90 °C for 3 h. The solvent was removed under vaccum and the residue was diluted with EtOAc. The organic phase was washed sequentially with $NaHCO_3$ (sat, aq), a solution of brine

(sat.), and water. The organic layer was dried over Na_2SO_4, filtered and evaporated. The crude product was purified by flash column chromatography (10%→50% 2-methylpentane in EtOAc) to give (1*R*,2*R*)-2-{4-[3-methyl-1-(tetrahydro-2*H*-pyran-2-yl)-1*H*-pyrazol-5-yl]benzoyl}-*N*-(4-oxo-4,5,6,7-tetrahydropyrazolo[1,5-*a*]pyrazin-3-yl)cyclohexanecarboxamide (1.0 g, 84 %) as a yellow solid. MS *m/z* 531 $[M+H]^+$.

*(1R,2R)-2-[4-(3-Methyl-1H-pyrazol-5-yl)benzoyl]-N-(4-oxo-4,5,6,7-tetrahydropyrazolo[1,5-a]pyrazin-3-yl)cyclohexanecarboxamide (**12**):* HCl (6 M in water, 20 mL) was added slowly to a solution of (1*R*,2*R*)-2-{4-[3-methyl-1-(tetrahydro-2*H*-pyran-2-yl)-1*H*-pyrazol-5-yl]benzoyl}-*N*-(4-oxo-4,5,6,7-tetrahydropyrazolo[1,5-*a*]pyrazin-3-yl)cyclohexanecarboxamide (3.5 g, 6.60 mmol) in dioxane (40 mL) and water (10 mL) at 4 °C over a period of 2 min. The reaction mixture was stirred at 5 min at 4 °C and was then allowed to reach rt and stirred for 1h. The solvent was removed under vaccum. The residue was diluted with a solution of Na_2CO_3 (sat, aq) and the aqueous layer was extracted three times with DCM. The solvent was removed under vaccum and the crude product was purified by reversed phase flash column chromatography (C18, 25→45%

CH_3CN in H_2O/HCO_2H, 99.9/0.1). Pure fractions were collected and evaporated to dryness to afford (1*R*,2*R*)-2-[4-(3-methyl-1*H*-pyrazol-5-yl)benzoyl]-*N*-(4-oxo-4,5,6,7-tetrahydropyrazolo[1,5-*a*]pyrazin-3-yl)cyclohexanecarboxamide (1.8 g, 61%) as a light yellow solid. ^{1}H NMR (600 MHz, DMSO) δ 12.75 (s, 1H), 9.14 (s, 1H), 8.31 (s, 1H), 7.96 – 8.06 (m, 2H), 7.81 – 7.92 (m, 3H), 6.56 (s, 1H), 4.16 – 4.25 (m, 2H), 3.68 – 3.76 (m, 1H), 3.59 (s, 2H), 2.92 – 3 (m, 1H), 2.28 (s, 3H), 2 – 2.07 (m, 1H), 1.92 – 2 (m, 1H), 1.71 – 1.84 (m, 2H), 1.33 – 1.56 (m, 3H), 1.12 – 1.22 (m, 1H); HRMS (ESI) m/z calcd for $C_{24}H_{26}N_6O_3$ $[M + H]^+$ 447.2142, found 447.2144.

ASSOCIATED CONTENT

Supporting Information

General synthetic information, ^{1}HNMR spectra for compounds **3-12**, protocols for DMPK, bioscience and safety assays, protocols for PK/PD studies, protocols for preclinical safety *in vivo* studies are available in the Supporting Information.

The following files are available free of charge:

AZD5718_JMC_Supporting Information

Molecular formula strings; FLAP binding IC_{50}; Human Whole Blood assay IC_{50}.

AUTHOR INFORMATION

Corresponding Author

* Daniel Pettersen

Cardiovascular, Renal and Metabolism IMED Biotech Unit,

AstraZeneca Gothenburg, Sweden

daniel.pettersen@astrazeneca.com

Tel: +46 (0)725899845

Present Addresses

Monika Sundqvist: Department of DMPK, Research, LEO Pharma A/S Industriparken 55

DK-2750 Ballerup, Denmark.

Alleyn T. Plowright: Integrated Drug Discovery, Sanofi-Aventis Deutschland GmbH, Industriepark Höchst, D-65926 Frankfurt am Main, Germany

Author Contributions

The manuscript was written through contributions of all authors. All authors have given approval to the final version of the manuscript. DP Medicinal chemistry lead and main author. JB Medicinal Chemist, HEm Medicinal Chemist, MAH DMPK design lead, ML Medicinal chemistry lead for earlier part of program, MSw Medicinal chemist, JU Computational chemist, CW Bioscience lead, CA PK/PD modelling, HEr Clinical PK/PD, AWE Preclinical safety lead, KG Medicinal chemistry contributions, ATP Medicinal chemistry contributions, IS Computational chemist Ames discussion partner, AD generation of FLAP binding data, MSu PK/PD modelling. MN, Preclinical Drug Metabolism and PK lead, ELL Project leader.

Funding Sources

The authors declare no competing financial interest.

ACKNOWLEDGMENT

Angela Menschik-Lundin, Anna Rönnborg and Bengt Kull for human whole blood data, Gun-Britt Forsberg for $uLTE_4$ analyses, Anne-Cristine Carlsson for the creatinine analyses in urine, Matt Skinner, Alex Harmer and Mike Rolf for safety pharmacology evaluation, Eike Floettmann for toxicology evaluation, Frank Seeliger for pathology evaluation, Marie Strimfors for dog PK and Ann-Sofie Sandinge for PK analysis, Thomas Elebring and Gabrielle Saarinen for compound syntheses, Staffan Karlsson for preclinical large scale chemistry and Tony Johansson for providing the cover art.

ABBREVIATIONS

5-LO 5-lipoxygenase; ACN acetonitrile; ACS acute coronary syndrome; ADME administration distribution metabolism excretion; CAD coronary artery disease; Cav3.2, human cardiac ion channel ICa_T; COX cyclooxygenase; CYP cytochrome P450; DCM dichloromethane; eD2M early dose to man prediction; FLAP 5-lipoxygenase activating protein; hBSEP, human Bile Salt Export Pump (ABCB11); HCN4, human cardiac ion channel IF; hIKs, human cardiac ion channel hKv7.1/hKCNE1; hIto, human cardiac ion

channel hKv4.3/hKChIP2.2; hKv1.5, human cardiac ion channel IKUR; hMrp2, human Multi-Drug Resistance Protein 2; hNav1.5, human cardiac channel INa; HepClint hepatic clearance intrinsic; hAhR, human aromatic hydrocarbon receptor, hWB human whole blood, LLE ligand lipophilic efficiency; LTA_4H leukotriene A_4 Hydrolase; LTB_4 leukotriene B_4; LTC_4S leukotriene C_4 Synthase; LTC_4 leukotriene C_4; LTD_4 leukotriene D_4; LTE_4 leukotriene E_4; LVEF left ventricular ejection fraction; NOEL no observed adverse effect level; PK/PD pharmacokinetic/pharmacodynamic; rt room temperature;

REFERENCES

1. Peters-Golden, M.; Henderson, W. R. Leukotrienes. *N.Eng. J. Med.* **2007,** 357, 1841-1854.

2. Haeggström, J. Z.; Funk, C. D. Lipoxygenase and leukotriene pathways: Biochemistry, biology, and roles in disease. *Chem. Rev.* **2011,** 111, 5866-5896.

3. Whatling, C.; McPheat, W.; Herslöf, M. The potential link between atherosclerosis and the 5-lipoxygenase pathway: Investigational agents with new implications for the cardiovascular field. *Expert Opin. Invest. Drugs* **2007,** 16, 1879-1893.

4. Tardif, J. C.; L'Allier, P. L.; Ibrahim, R.; Grégoire, J. C.; Nozza, A.; Cossette, M.; Kouz, S.; Lavoie, M. A.; Paquin, J.; Brotz, T. M.; Taub, R.; Pressacco, J. Treatment with 5-lipoxygenase inhibitor VIA-2291 (atreleuton) in patients with recent acute coronary syndrome. *Circulation: Cardiovascular Imaging* **2010,** 3, 298-307.

5. Ahmadi, N.; Budoff, M.; Tabibiazar, R.; Craves, F.; Brotz, T. Methods For Treating Cardiovascular Diseases. WO2014031586 (A2) **2014**.

6. Gaztanaga, J.; Farkouh, M.; Rudd, J. H. F.; Brotz, T. M.; Rosenbaum, D.; Mani, V.; Kerwin, T. C.; Taub, R.; Tardif, J.-C.; Tawakol, A.; Fayad, Z. A. A phase 2 randomized, double-blind, placebo-controlled study of the effect of VIA-2291, a 5-lipoxygenase inhibitor, on vascular inflammation in patients after an acute coronary syndrome. *Atherosclerosis* **2015,** 240, 53-60.

7. Hu, C.; Ma, S. Recent development of lipoxygenase inhibitors as anti-inflammatory agents. *MedChemComm* **2018,** 9, 212-225.

8. Bruno, F.; Spaziano, G.; Liparulo, A.; Roviezzo, F.; Nabavi, S. M.; Sureda, A.; Filosa, R.; D'Agostino, B. Recent advances in the search for novel 5-lipoxygenase inhibitors for the treatment of asthma. *Eur. J. Med. Chem.* **2018,** 153, 65-72.

9. Evans, J. F.; Ferguson, A. D.; Mosley, R. T.; Hutchinson, J. H. What's all the FLAP about? 5-Lipoxygenase-activating protein inhibitors for inflammatory diseases. *Trends Pharmacol Sci* **2008,** 29, 72-78.

10. Pettersen, D.; Davidsson, Ö.; Whatling, C. Recent advances for FLAP inhibitors. *Bioorgan. Med. Chem. Lett.* **2015,** 25, 2607-2612.

11. Stock, N. S.; Bain, G.; Zunic, J.; Li, Y.; Ziff, J.; Roppe, J.; Santini, A.; Darlington, J.; Prodanovich, P.; King, C. D.; Baccei, C.; Lee, C.; Rong, H.; Chapman, C.; Broadhead, A.; Lorrain, D.; Correa, L.; Hutchinson, J. H.; Evans, J. F.; Prasit, P. 5-Lipoxygenase-activating protein (FLAP) Inhibitors. Part 4: Development of 3-[3-tert-Butylsulfanyl-1-[4-(6-ethoxypyridin-3-yl)benzyl]-5-(5-methylpyridin-2-ylmethoxy)-1H-indol-2-yl]-2,2-dimethylpropionic Acid (AM803), a potent, oral, once daily FLAP inhibitor. *J. Med. Chem.* **2011,** 54, 8013-8029.

12. Takahashi, H.; Bartolozzi, A.; Simpson, T. Discovery of the Novel Oxadiazole Containing 5-Lipoxygenase Activating Protein (FLAP) Inhibitor BI 665915. In *Comprehensive Accounts of Pharmaceutical Research and Development: From Discovery to Late-Stage Process Development Volume 1*, American Chemical Society: ACS eBook, 2016; Vol. 1239, pp 101-119.

13. Gür, Z. T.; Çalışkan, B.; Banoglu, E. Drug discovery approaches targeting 5-lipoxygenase-activating protein (FLAP) for inhibition of cellular leukotriene biosynthesis. *Eur. J. Med. Chem.* **2018,** 153, 34-48.

14. Ferguson, A. D.; McKeever, B. M.; Xu, S.; Wisniewski, D.; Miller, D. K.; Yamin, T. T.; Spencer, R. H.; Chu, L.; Ujjainwalla, F.; Cunningham, B. R.; Evans, J. F.; Becker, J. W. Crystal structure of inhibitor-bound human 5-lipoxygenase-activating protein. *Science* **2007,** 317, 510-512.

15. Prasit, P.; Belley, M.; Blouin, M.; Brideau, C.; Chan, C.; Charleson, S.; Evans, J.; Frenette, R.; Gauthier, J.; Guay, J. J. J. o. l. m. A new class of leukotriene biosynthesis inhibitor: the development of MK-0591. *J. Lipid. Mediat.* **1993,** 6, 239-244.

16. Lemurell, M.; Ulander, J.; Winiwarter, S.; Dahlén, A.; Davidsson, Ö.; Emtenäs, H.; Broddefalk, J.; Swanson, M.; Hovdal, D.; Plowright, A. T.; Pettersen, A.; Rydén-Landergren, M.; Barlind, J.; Llinas, A.; Herslöf, M.; Drmota, T.; Sigfridsson, K.; Moses, S.; Whatling, C. Discovery of AZD6642, an inhibitor of 5-lipoxygenase activating protein (FLAP) for the treatment of inflammatory diseases. *J. Med. Chem.* **2015,** 58, 897-911.

17. Lemurell, M.; Ulander, J.; Emtenäs, H.; Winiwarter, S.; Broddefalk, J.; Swanson, M.; Hayes, M. A.; Garcia, L. P.; Westin Eriksson, A.; Cassel, J.; Saarinen, G.; Yuan, Z.-Q.; Löfberg, C.; Karlsson, S.; Sundqvist, M.; Whatling, C. A novel chemical series of 5-LO activating protein (FLAP) inhibitors for treatment of Coronary Artery Disease. *J. Med.Chem.* **2018,** *In press*.

18. Banoglu, E.; Çalışkan, B.; Luderer, S.; Eren, G.; Özkan, Y.; Altenhofen, W.; Weinigel, C.; Barz, D.; Gerstmeier, J.; Pergola, C.; Werz, O. Identification of novel benzimidazole derivatives as inhibitors of leukotriene biosynthesis by virtual screening targeting 5-lipoxygenase-activating protein (FLAP). *Bioorg.Med.Chem.* **2012,** 20, 3728-3741.

19. Folco, G.; Murphy, R. C. Eicosanoid transcellular biosynthesis: From cell-cell interactions to in vivo tissue responses. *Pharmacol. Rev.* **2006,** 58, 375-388.

20. Turesky, R. J. Aromatic Amines and Heterocyclic Aromatic Amines: From Tobacco Smoke to Food Mutagens. In The Chemical Biology of DNA Damage (pp. 157-183) **2010**. Wiley-VCH. https://doi.org/10.1002/9783527630110.ch7.

21. Kim, D.; Guengerich, F. P. Cytochrome P450 activation of arylamines and heterocyclic amines. *Ann. Rev.Pharmacol.Tox.* **2004,** 45, 27-49.

22. Ames, B. N.; McCann, J.; Yamasaki, E. Methods for detecting carcinogens and mutagens with the salmonella/mammalian-microsome mutagenicity test. *Mutation Research/Environmental Mutagenesis and Related Subjects* **1975,** 31, 347-363.

23. Ripa, L.; Mee, C.; Sjö, P.; Shamovsky, I. Theoretical studies of the mechanism of N-hydroxylation of primary aromatic amines by cytochrome P450 1A2: Radicaloid or anionic? *Chem. Res. Tox.* **2014,** 27, 265-278.

24. Shamovsky, I.; Ripa, L.; Börjesson, L.; Mee, C.; Nordén, B.; Hansen, P.; Hasselgren, C.; O'Donovan, M.; Sjö, P. Explanation for main features of sructure–genotoxicity relationships of aromatic amines by theoretical studies of their activation pathways in CYP1A2. *J. Am. Chem. Soc.* **2011,** 133, 16168-16185.

25. Shamovsky, I.; Ripa, L.; Blomberg, N.; Eriksson, L. A.; Hansen, P.; Mee, C.; Tyrchan, C.; O'Donovan, M.; Sjö, P. Theoretical studies of chemical reactivity of metabolically activated forms of aromatic amines toward DNA. *Chem.Res. Tox.* **2012,** 25, 2236-2252.

26. Blevitt, J. M.; Hack, M. D.; Herman, K.; Chang, L.; Keith, J. M.; Mirzadegan, T.; Rao, N. L.; Lebsack, A. D.; Milla, M. E. A single amino acid difference between mouse and human 5-lipoxygenase activating protein (FLAP) explains the speciation and differential pharmacology of novel FLAP Inhibitors. *J. Biol. Chem.* **2016,** 291, 12724-12731.

27. Øie, S.; Tozer, T. N. Effect of altered plasma protein binding on apparent volume of distribution. *J.Pharm. Sci.***1979,** 68, 1203-1205.

28. Ericsson, H.; Nelander, K.; Lagerstrom-Fermer, M.; Balendran, C.; Bhat, M.; Chialda, L.; Gan, L.-M.; Heijer, M.; Kjaer, M.; Lambert, J.; Lindstedt, E.-L.; Forsberg, G.-B.; Whatling, C.; Skrtic, S. Initial clinical experience with AZD5718, a novel once daily oral 5-lipoxygenase activating protein inhibitor. *Clin.Trans. Sci.* **2018,** 11, 330-338.

29. Bain, G.; King, C. D.; Rewolinski, M.; Schaab, K.; Santini, A. M.; Shapiro, D.; Moran, M.; van de Wetering de Rooij, S.; Roffel, A. F.; Schuilenga-Hut, P.; Milne, G. L.; Lorrain, D. S.; Li, Y.; Arruda, J. M.; Hutchinson, J. H.; Prasit, P.; Evans, J. F.

Pharmacodynamics and pharmacokinetics of AM103, a novel inibitor of 5-lipoxygenase-activating protein (FLAP). *Clin.Pharmacol.Ther.* **2010,** 87, 437-444.

30. Karlsson, S.; Bergman, R.; Broddefalk, J.; Löfberg, C.; Moore, P. R.; Stark, A.; Emtenäs, H. A practical telescoped three-step sequence for the preparation of (1*R*,2*R*)-2-(4-bromobenzoyl)cyclohexanecarboxylic acid: A key building block used in one of our drug development projects. *Org. Process Res. Dev.* **2018,** 22, 618-624.

Table of Contents graphic

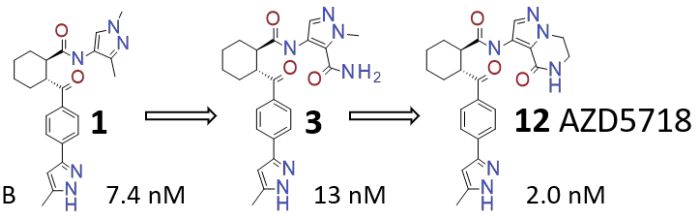

	1	3	12 AZD5718
FLAP IC_{50free} hWB	7.4 nM	13 nM	2.0 nM
Ames free amino-pyrazole	**Yes**	**No**	**Yes**
Early dose to man pred.	1900 mg	170 mg	**44 mg**
CV safety (dog)	**20x margin**	NT	**No adverse effects (>120x C_{max})**

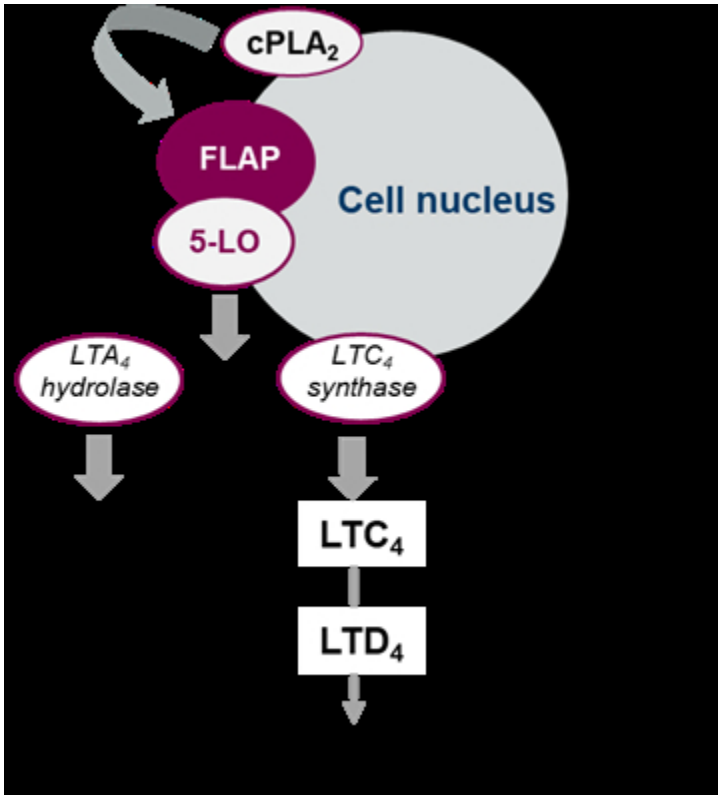

94x104mm (96 x 96 DPI)

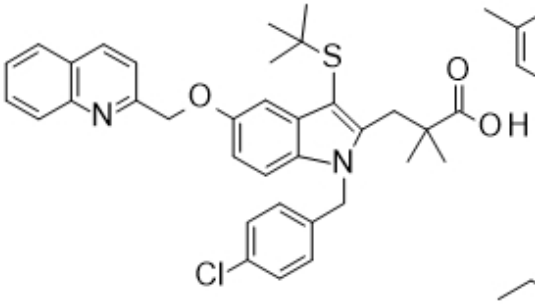

MK-591

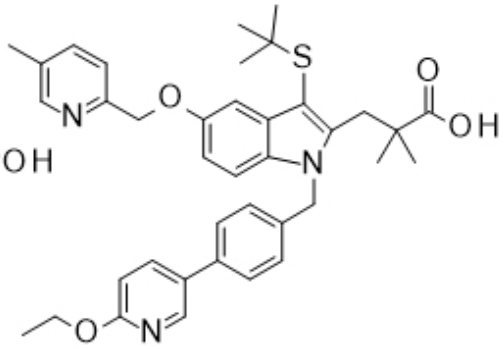

AM803

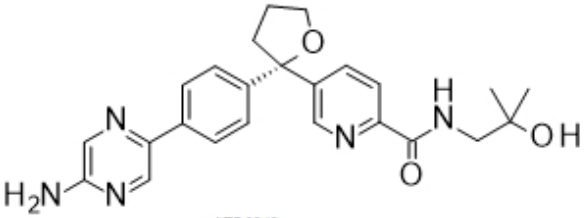

AZD6642

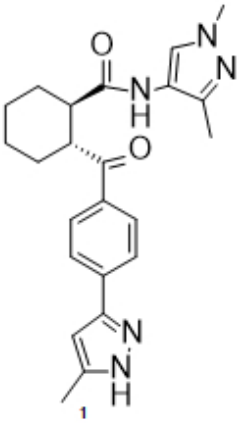

1

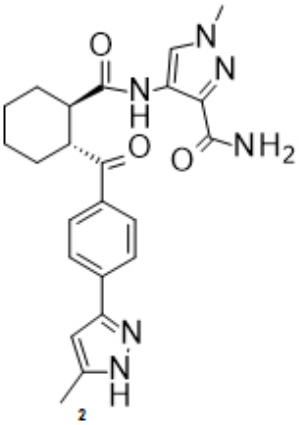

2

134x154mm (96 x 96 DPI)

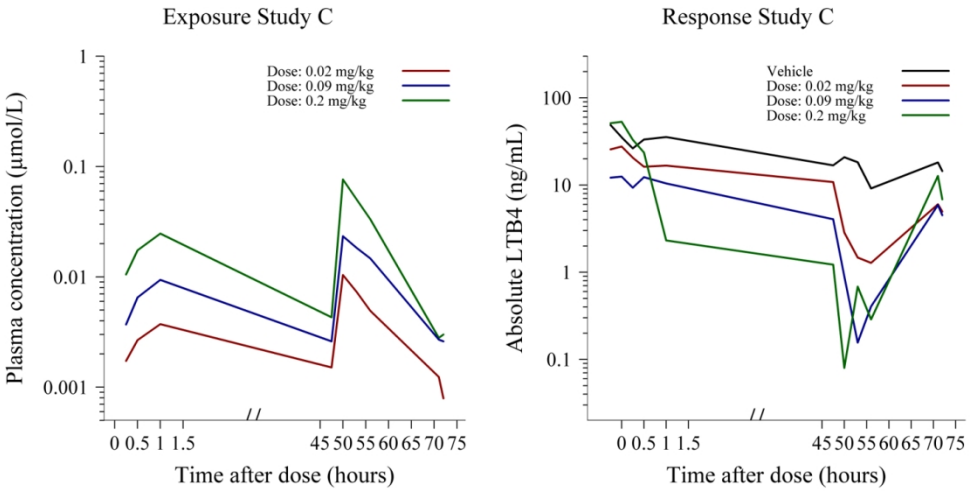

254x126mm (150 x 150 DPI)

112x95mm (96 x 96 DPI)

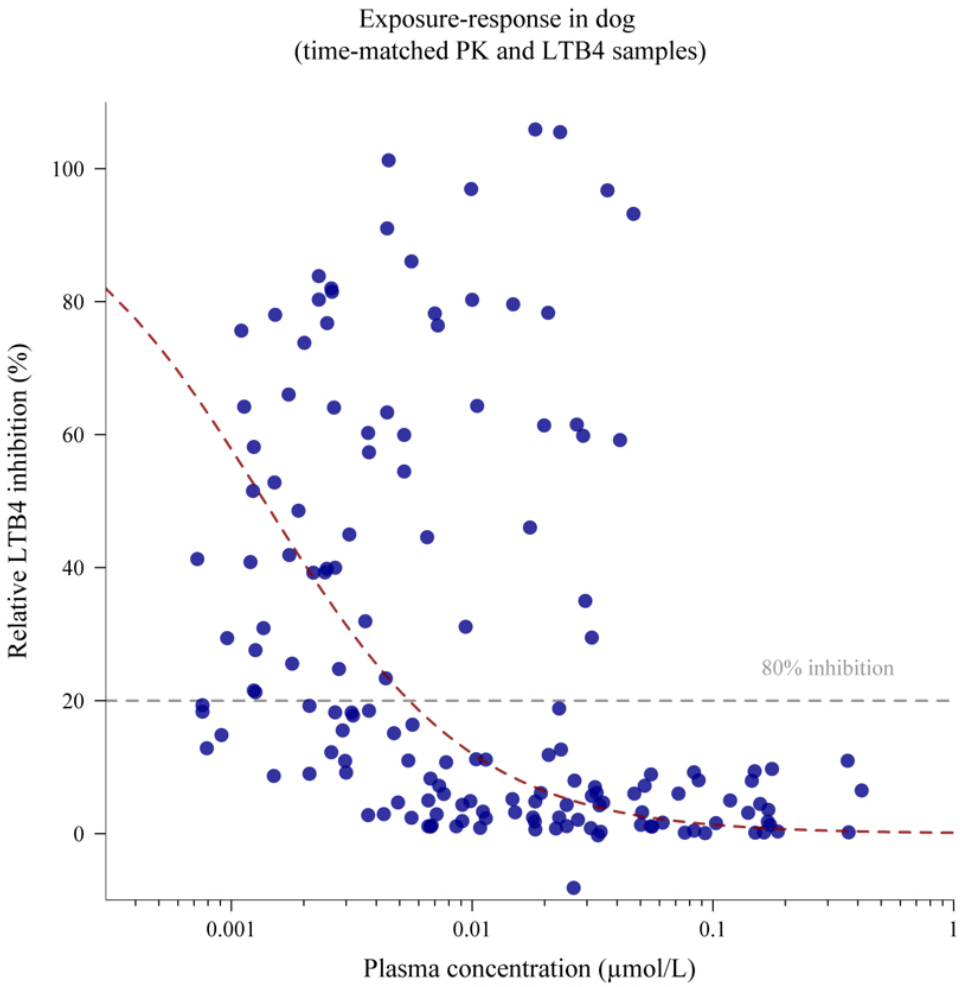

142x142mm (150 x 150 DPI)

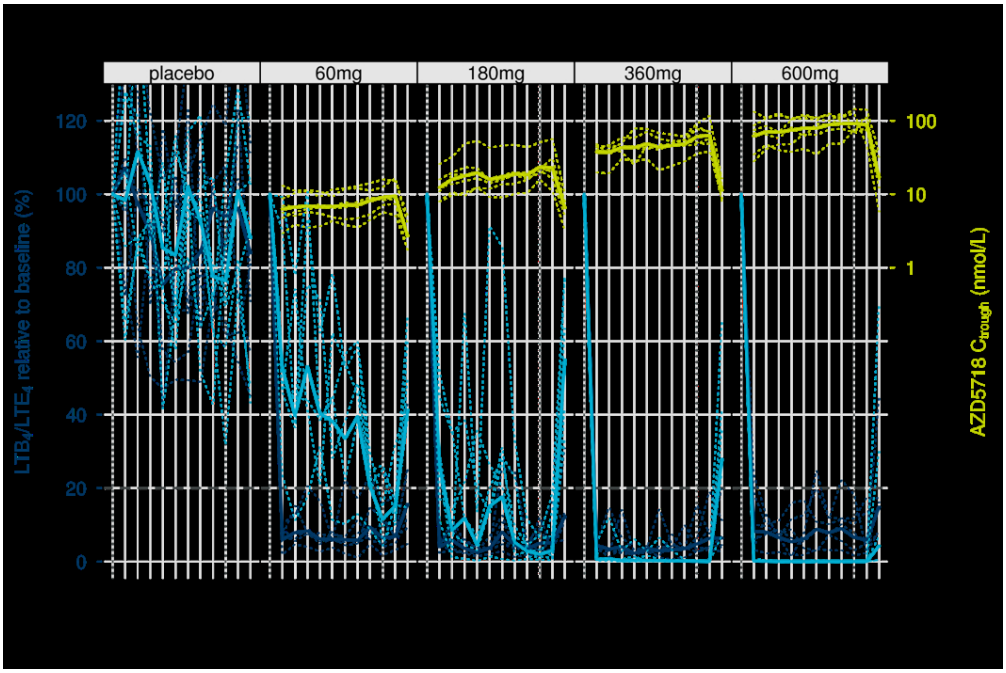

179x119mm (150 x 150 DPI)

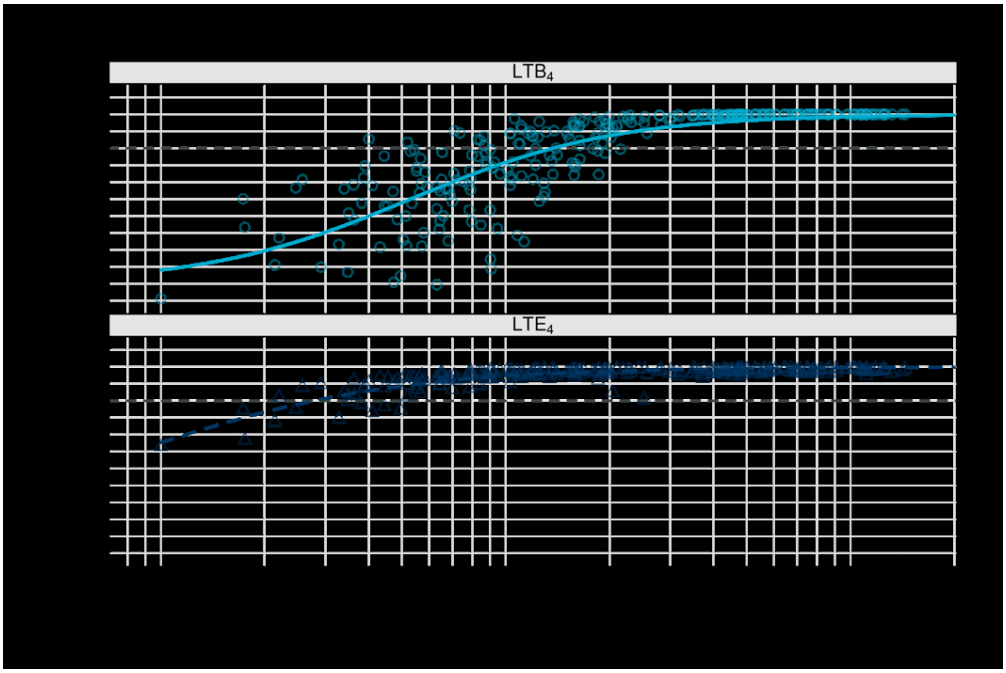

179x119mm (150 x 150 DPI)

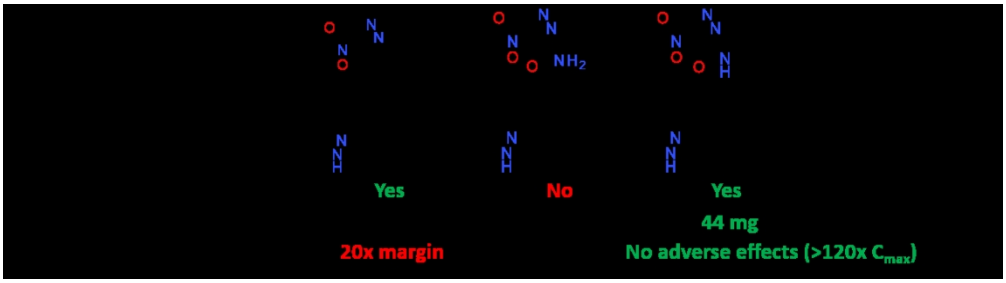

218x59mm (150 x 150 DPI)